J 20 419 F

A Publication for the Radio-Amateur

Especially Covering VHF, UHF and Microwaves

VHF communications

Volume No.17 · Autumn · 3/1985 · DM 7.00

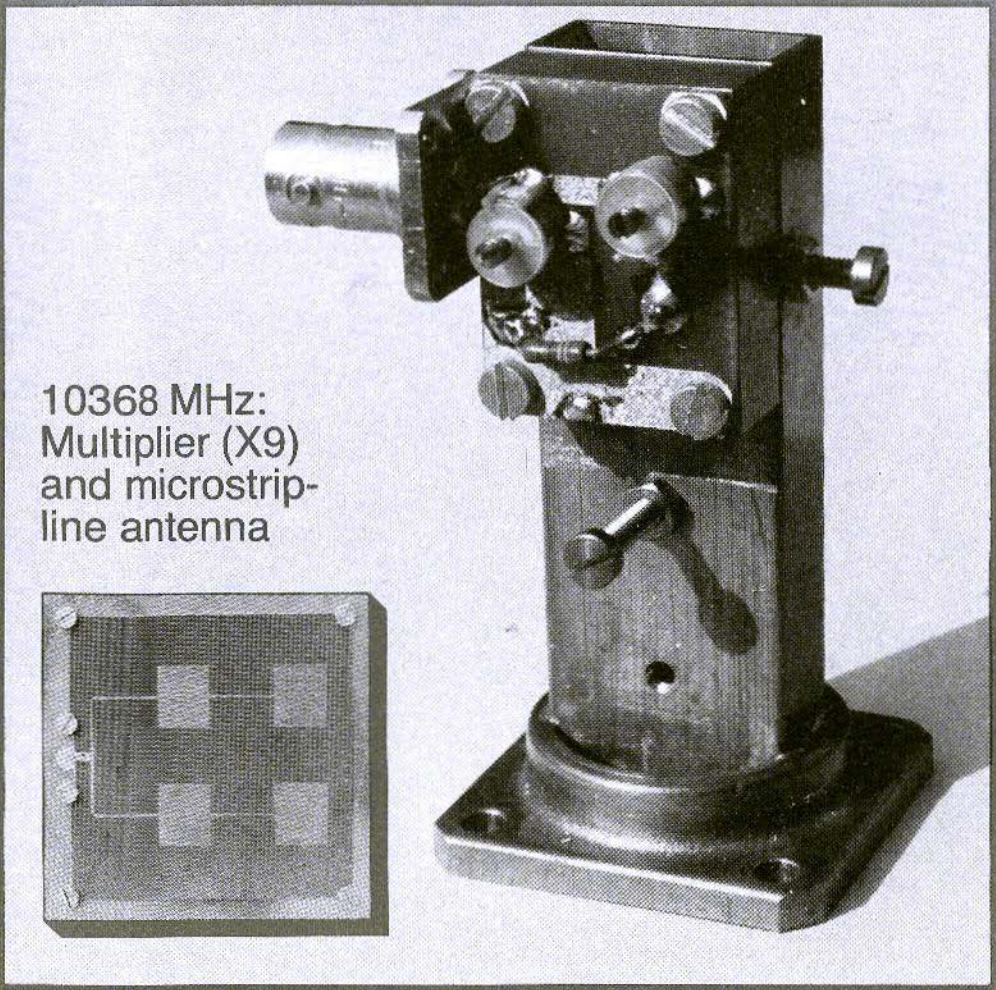

10368 MHz: Multiplier (X9) and microstrip-line antenna

VHF communications

A Publication for the Radio Amateur
Especially Covering VHF, UHF, and Microwaves

Volume No. 17 · Autumn · Edition 3/1985

Published by: Verlag UKW-BERICHTE,
Terry Bittan
Jahnstrasse 14
D-8523 BAIERSDORF
Fed. Rep. of Germany
Telephone (9133) 855
Telex 629 887
Postgiro Nbg. 30455-858

Publisher: Verlag UKW-TECHNIK
Terry Bittan

Editors: Corrie Bittan
Colin J. Brock (Assistant)

Translator: Colin J. Brock
G 3 ISB/DJ Ø OK

Advertising manager: Corrie Bittan

VHF COMMUNICATIONS The international edition of the German publication UKW-BERICHTE, is a quarterly amateur radio magazine especially catering for the VHF/UHF/SHF technology. It is published in Spring, Summer, Autumn, and Winter. The 1985 subscription price is DM 24.00 or national equivalent per year. Individual copies are available at DM 7.00 or equivalent, each. Subscriptions, orders of individual copies, purchase of PC-boards and advertised special components, advertisements and contributions to the magazine should be addressed to the national representative, or – if not possible – direct to the publishers.

Printed in the Fed. Rep. of Germany by R. Reichenbach KG. Krelingstr. 39 · 8500 Nuernberg.

We would be grateful if you would address your orders and queries to your representative.

Representatives

Austria
Verlag UKW-BERICHTE, Terry D. Bittan
POB 80, D-8523 Baiersdorf/W.Germany
Creditanstalt Bankverein, WIEN Kto. 17-90.599;
PSchKto WIEN 1.169.146

Australia
W.I.A. P.O.Box 300, South Caulfield, 3162 VIC. Phone 5285962

Belgium
HAM INTERNATIONAL, Brusselsesteenweg 428, B-9218 GENT,
PCR 000-1014257 CCP, Tel.00-32-91-312111

Denmark
Halskov Electronic, OZ7LX, Sigersted gamle Skole,
DK-4100 RINGSTED. Telf. 03-616162, Giro 7 29 68 00

France
Christiane Michel, F 5 SM, SM Electronic,
20 bis, Avenue des Clairions, F-89000 AUXERRE
Tel.(86) 46 96 59

Finland
Erkki Hohenthal, SF-31400 SOMERO
Joensuuntie 6, Tel. 924-46311

Holland
MECOM, PA 0 AER, Postbus 40, Noordwalderweg 12,
NL-9780 AA BEDUM, Tel. 05900-14390,
Postgiro 3986163

Israel
Z. Pomer, 4X4KT, PO Box 222, K. MOZKIN 26114
Tel. 00972-4714078

Italy
Franco Armenghi, I 4 LCK, Via Sigonio 2,
I-40137 BOLOGNA, Tel.(051) 34 66 97

Luxembourg
TELECO, Jos. Faber, LX 1 DF, 5–9, Rue de la fontaine,
ESCH-SUR-ALZETTE, Tel. 53752

New Zealand
E. M. Zimmermann, ZL 1 AGQ, PO Box 31-261
Milford, AUCKLAND 9, Phone 492-744

Norway
Henning Theg, LA 4 YG, Postboks 70,
N-1324 LYSAKER, Postgirokonto 3 16 00 09

South Africa
SA Radio Publications, PO Box 2232, JOHANNESBURG 2000, Telephone 011-3378472

Spain + Portugal
Julio A. Prieto Alonso, EA 4 CJ, MADRID-15,
Donoso Cortes 58 5°-B, Tel. 243.83.84

Sweden
Carl-Oscar Biese, SM4IVL, Gjuteribacken 12 B
S-17239 SUNDBYBERG, Tel. 08-29 63 22

Switzerland
Terry Bittan, Schweiz, Kreditanstalt ZÜRICH,
Kto.469.253-41; PSchKto ZÜRICH 80-54.849

USA
UV COMMS, K3BRS
PO Box 432, LANHAM, MD 20706
Tel. 301-459-4924

ISSN 0177-7505

Contents

Alois Aigner, DL 6 XE	**Helical Antenna for the 70 cm Band**	130 - 132
Wolfram Pueschner, DF 7 KB	**The Noise Behaviour of Amplifiers**	133 - 137
Joachim Kestler, DK 1 OF	**PLL-Oscillators with Delay-Lines Part 4: Carrier Noise Sidebands**	138 - 140
Horst Burfeindt, DC 9 XG	**GaAs-FET Inter-Locked Dual-Polarity Power Supplies for portable Use**	141 - 145
Jochen Jirmann, DB 1 NV	**A Stable Crystal-Controlled-Source for 10,37 GHz**	146 - 152
Erich Stadler, DG 7 GK	**Measurement of Cable-Impedance with Impulses and Sine-Waves**	153 - 157
Gerd Körner, DK 2 LR	**The PCB-Integrated Coaxial Tuned Circuit**	158 - 160
Jochen Jirmann, DB 1 NV	**A 12-V-Mobile, Switched-Mode Power Supply (SMPS) Part 3 (Concluding)**	161 - 168
Drs. Tjapke Knoeff, PAØ	**FM/AM Converter for Facsimile Reception and Picture Display with the YU3UMV Picture-Store**	169 - 172
Matjaž Vidmar, YU 3 UMV	**Polarization Performance of Circularly Polarized Antennas**	173 - 177
ErichStadler, DG 7 GK	**The Directional Function and Use**	178 - 184
Bernd von Bojan, DJ 7 YE	**Determination of Antennas Gain – What's actually behind it all?**	185 - 191

Dear Reader!

Firstly, the staff of VHF COMMUNICATIONS wishes all subscribers and readers a very **Happy** and **Prosperous New Year**.

At the same time we would like to introduce our new translator Colin J. Brock.

He is an Englishman, working as a Tropospheric Scatter Systems Engineer in Germany and is a radio-amateur under the current license G3ISB/DJØOK.

Owing to his spontaneous participation, we were abie to rescue VHF COMMUNICATIONS. We are eagerly preparing edition 4 of this volume and are sure that you too, are looking forward to it. We hope that our subscribers will excuse the delay and support us again in the future.

Yours, Corrie Bittan

Alois Aigner, DL 6 XE

Helical Antenna for the 70 cm Band

From the standpoint of the publication (1) of the 23 cm band helical antenna by Hans-Jürgen Griem DJ1SL, I would like to briefly describe a version for the 70 cm band. At the same time I would like to give to anyone interested, the encouragement to take this uncritical, weekend project in hand. The actual constructional effort isn't much, it's just the will required to do-it-yourself. I use the helical antenna for the reception of the L-band transponder for Oscar 10 and together with a low-noise pre-amplifier I get good readable low-noise signals.

Originally, the 70 cm helical antenna published in 1974 by Wolfgang Stich, OE1GHB(2), was considered but finally the conical form and above all, the simple matching of the DJ1SL-version appeared to me to be a significant step forward. From (2) however, the spacing of the supports was obtained.

Enough now of the preliminaries - the following material is required for a 70 cm helical antenna: -

- A 2,5 m long alu support tube (boom including fixing), and of 30 x 30 mm (about) square cross-section
- 30 plastic insulators (helix supports)
- about 11 m of wire (e.g. 4mm dia Cu. lacquered)
- a metal sheet (of alu) for the reflector
- the will to build an antenna

Fig. 1 shows the external dimensions of the 70 cm helical antenna.

Now proceed in the following order: -

- Measure the spacings for the insulators and mark their positions along the boom. Bore the holes (the same dia. as the insulator); as shown in **fig. 3.**
- Cut the insulators **(fig. 2)** and drill the fixing and helix holes.
- Wind the wire on 200 mm dia. tube thus forming the helix.
- Thread the wire through the insulators.

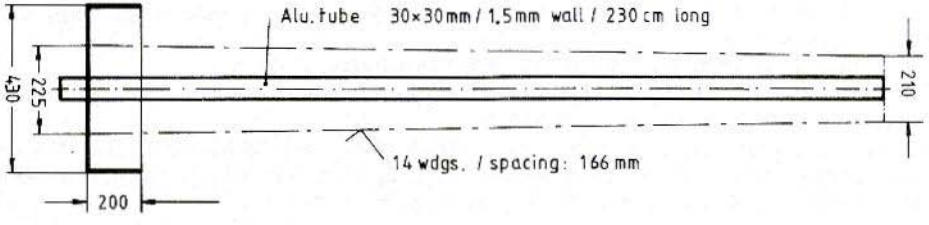

Fig. 1: Overall dimensions of the 70 cm helical antenna

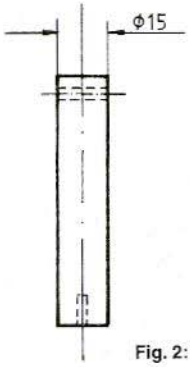

Fig. 2: Insulator/support

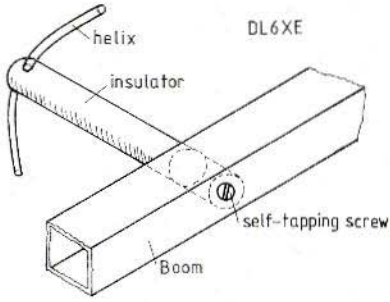

Fig. 3: Fixing together boom, insulator and helix

- Fasten the insulators to the boom.
- Saw-out a round reflector disc from sheet alu. with a jig-saw and fit a 200 mm alu. strip edging by means of brackets or welding.
- Fix an N panel-mounting socket (at the end of the helix) in the reflector disc and mount a λ/4 metal strip with an adjustment screw as in **figs. 4 and 5.**
- Point the antenna skywards and with a 70 cm signal generator and reflectometer adjust for optimal results by bending the strip and fine-adjusting the screw (remember to lock the screw).

The concluding photo series shows the formation of the antenna very clearly.

Materials

Boom from 30 x 30 mm square section alu. stock (hobby shops)
Insulators: tubular-polyamid PA 11/12 from Mssrs. Thyssen-Schulte GmbH
Tel.: Munich 089 - 41531, Linz: 732 - 74333

References

(1) Griem, H.-J., DJ 1 SL
A Helical Antenna for the 23 cm Band
VHF Comm. Vol. 15. 1983 ed. 3
Pages 184 - 189

(2) Stich, W., OE 1 GHB
A Helical Antenna for the 70 cm Band
VHF Comm. Vol. 6. 1974 ed. 3
Pages 149 - 155

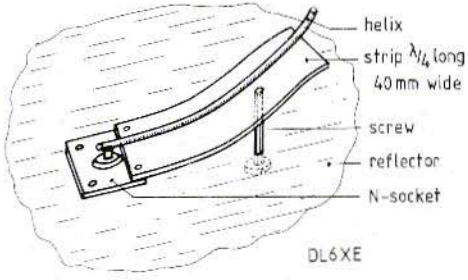

Fig. 4: Arrangement for matching helix to cable Zo

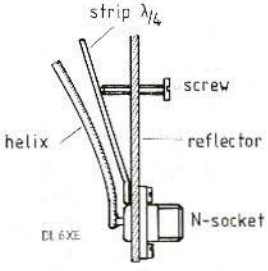

Fig. 5: Matching arrangement-side view

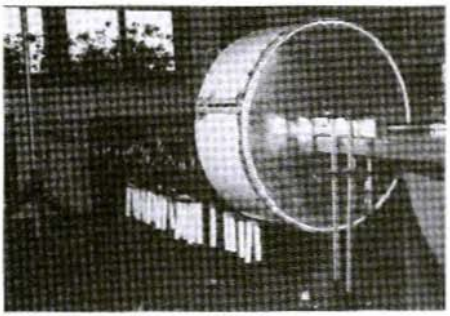

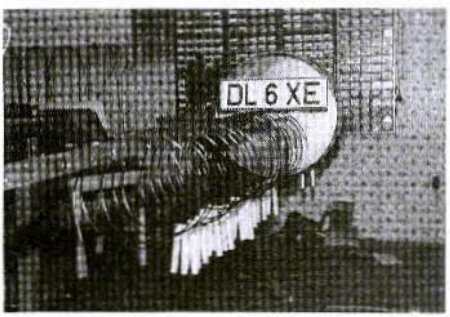

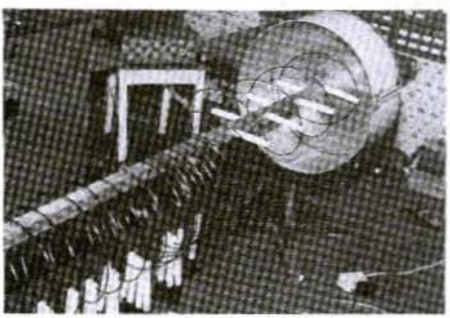

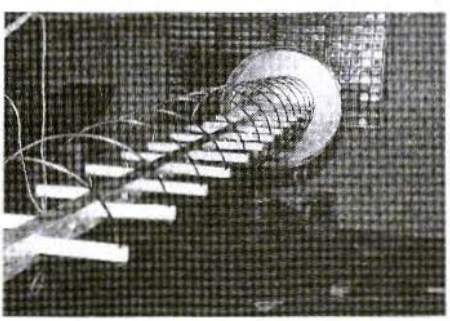

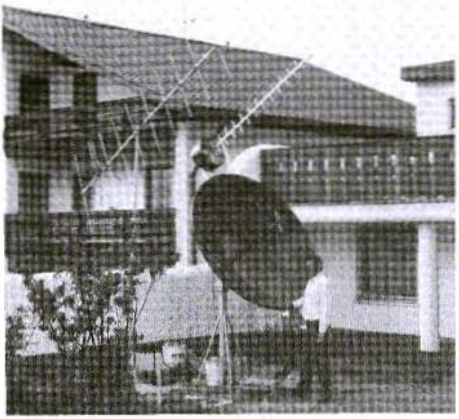

Fig. 6 - 12: The constructional development of the author's helical antenna

Wolfram Pueschner, DF 7 KB

The Noise Behaviour of Amplifiers

This article describes some experiments and results in the theme noise and noise-matching of antenna pre-amplifiers.

In communication technology, the relationship $R_i = Z_0 = Z_{ant}$ for optimum power transfer is well known. This is described as matching, that is, the generator/load resistance (e.g. antenna) equals the characteristic impedance of the antenna cable and that of the input/output impedance of the receiver/transmitter.

Unfortunately, the observance of the conditions for matching a receiver input stage usually do not achieve the optimum signal to noise ratio. For minimum noise the input tuned circuit of the first stage must be mistuned with respect to the point of maximum gain. This means however, that one of the matching conditions concerning the input impedance of the amplifier has been violated. **Fig. 1** makes this relationship clear. The values used in **Fig. 1** were taken from an actual 70 cm band amplifying stage, shown in **Fig. 2**. The measurement tolerances are +/– 0,25 dB. Noise figure values well below 1 dB are easily possible with relatively little outlay (**see Fig. 3**).

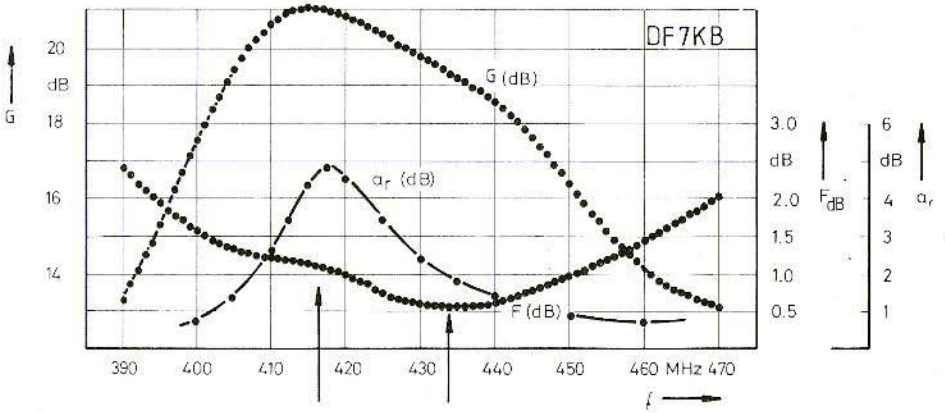

Fig. 1: Test results from a 70 cm pre-amplifier using a 3SK97 adjusted for minimum noise
Gain = G return loss = a_r Noise figure = F_{dB}
Test equipment: Sweeper SWOB5 and noise figure meter HP 8970A
Left arrow: Indentation probably caused by regulation effect of NF-meter (G > 20 dB)
Right arrow: Noise matching at 432 MHz

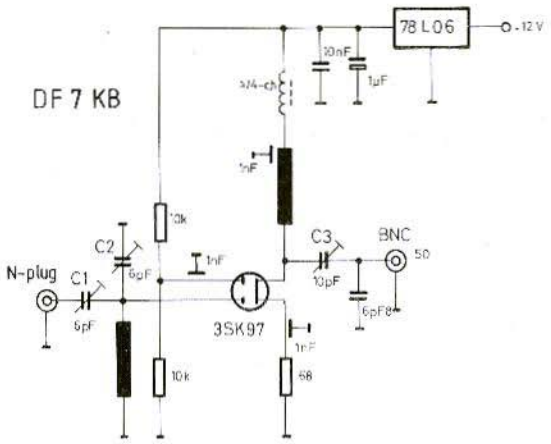

Fig. 2: 70 cm pre-amp. used as test-item. By adjusting the source resistance minimum noise may be obtained

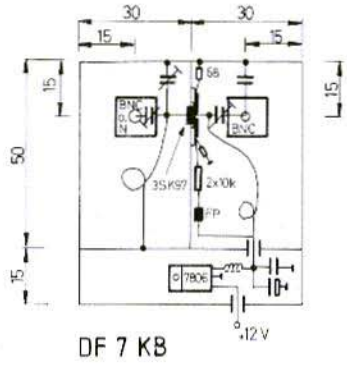

Fig. 3: Constructional sketch of 70 cm pre-amp. All internal measurements

The same amplifier was constructed again but this time with high quality input trimmers (Johanson and Glasrohr) and in a brass housing. A considerable improvement however, was not to be obtained. A discernible noise minimum however was obtained in the two versions, by altering the drain current for best results.

In order to clarify the relationship between noise-matching and power-matching, the same amplifier was adjusted for a maximum return-loss a_r and maximum gain G. The noise worsened at 432 MHz from 0,6 dB to 1,2 dB (**Fig. 4**). Minimum noise was now obtained at 450 MHz.

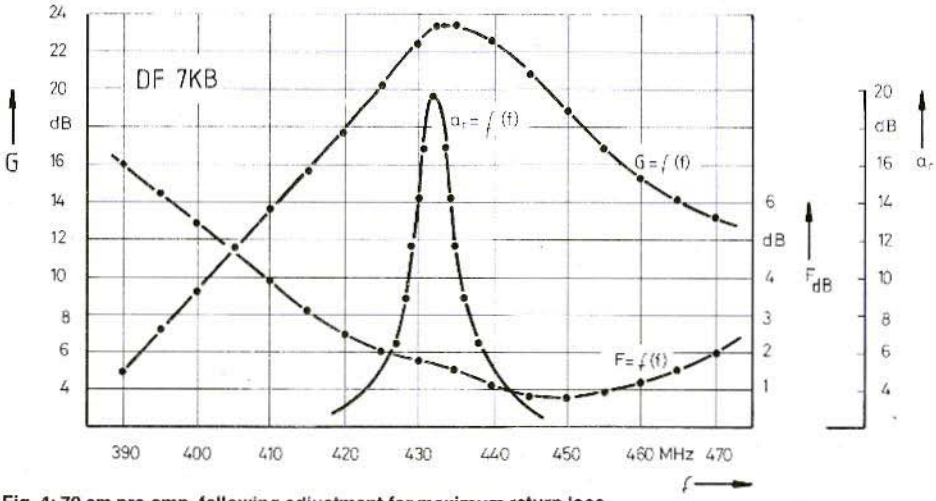

Fig. 4: 70 cm pre-amp. following adjustment for maximum return loss. Test set-up as in fig. 1

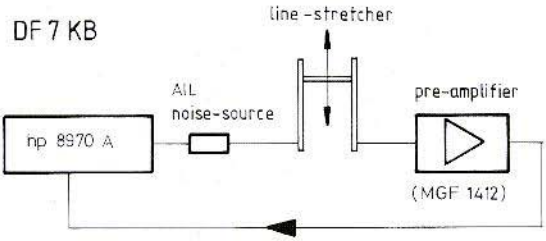

Fig. 5:
Test set-up to determine the relationship between noise-figure and gain of a pre-amp. and the line length between amplifier and generator

Figs. 1 and 4 show that an amplifier's noise minimum is not to be obtained by power matching. If the input impedance departs from the system characteristic impedance (say 50 Ω) then this input impedance will be transformed to a value which is dependent upon the electrical length of any section of line which is connected to it. Transmission line theory will then determine the required result.

The input impedance of a line in dependence upon its length, the reflection factor at the end of the line, and the characteristic impedance, results in a function which shows a spiral form in the characteristic of the input impedance versus the line length.

This means that the choice of line section before the amplifier can always be used to transform the impedance to almost any desired value. A total mismatch with the appropriate losses is possible but so is the optimum noise match between generator (ant.) and amplifier achieved by means of the suitable choice of cable length.

The following extract will describe a measurement in which the noise figure and the gain of a pre-amplifier is demonstrated to be dependent upon the line length connecting amplifier to generator. An adjustable length line (line stretcher) is necessary (**Fig. 5**). The mathematical function of the complex input impedance of a line shows a periodicity of λ/2. The line length is therefore required to be variable above the range of λ/2.

A coaxial line-stretcher was available with a length variation of only 120 mm. The foregoing description of a 70 cm pre-amplifier was therefore not suitable for the experiment. The experiments were therefore conducted in the 23 cm band using a MGF 1412 amplifier (**Fig. 6**). The salient particulars of this amplifier are:

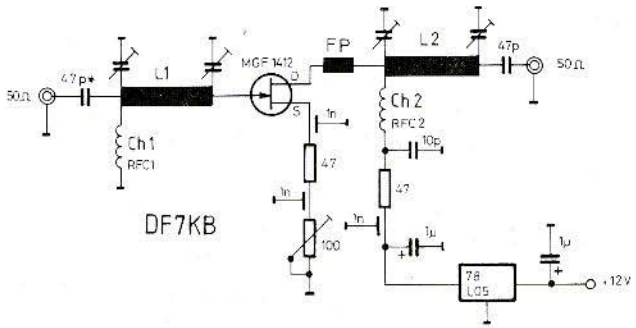

Fig. 6:
A low-noise 23 cm pre-amp. with GaAs-FET for further experiments

L 1: Silvered brass strip (25 x 10 x 0,5) mm
L 2: ditto but 21 mm long
Ch 1: 9 windings 0,3 mm Cu-lacquered wire 3 mm former
Ch 2: 2 windings silvered 1 mm wire on 5 mm former
Trimmers: Johanson 6 pF
Capacitors: All shown with * are disc ceramics

The HP 8970 A noise figure meter is a direct reading instrument which reads both the amplification and the noise-figure of the item-under-test (IUT) in decibels. Prior to the measurement the amplifier is connected to a noise source and adjusted for a noise minimum at 1296 MHz.

The following results were obtained:
G = 16,3 dB
F_{dB} = 0,25 dB
(Instrument measurement tolerance = +/− 0,25 dB)

As one of those on the brink of remarkable facts, was displayed by the prototype MGF 1412 amplifier. The transformation elements were originally fitted with standard tubular trimmers. The lowest obtainable noise figure was about 1,2 dB but only following the replacement of the two input trimmers by those made by Johanson.

Fig. 7 shows the dependence of the gain and the noise figure upon the line length between noise-source and amplifier input. The periodicity is clearly recognisable, again the length between minima/maxima being λ/2.

The minimum noise figure departed a little from that directly obtainable from the noise generator output terminals owing to the insertion loss of the line-stretcher. The change in attenuation owing to the alteration in line length of the line-stretcher was not taken into account. Errors due to this source are however, so small that they can be neglected in this application.

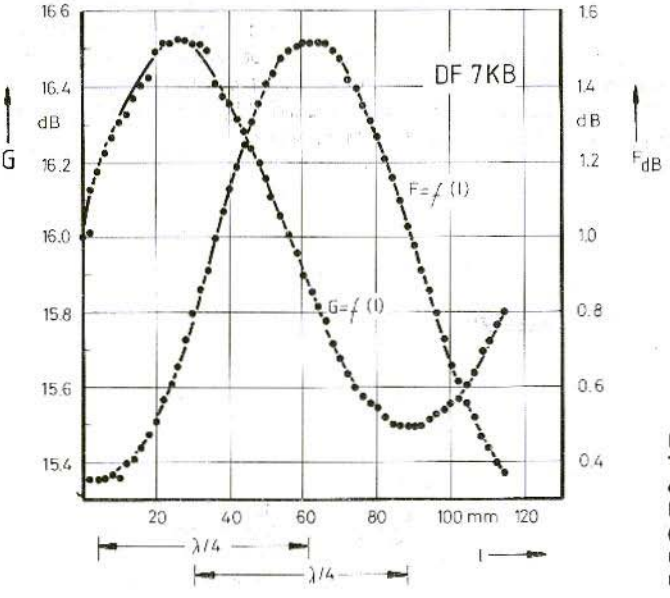

Fig. 7:
Test results for the amplifier of fig. 6 show that by a suitable line-length between generator (ant.) and pre-amplifier the minimal system noise-figure may be realised

The variation in noise-figure between about 0,35 dB and 1,5 dB due to a change in line length of about 60 mm ($\lambda/4$ at 1296 MHz = 57,8 mm) is worthy of note.

The change in noise figure with line length depends upon the relationship between the test equipment source impedance and that of the noise matched impedance of the semi-conductor under test. Some of the later bipolar transistors e.g. BFQ 69 display a noise minimum of near 70 Ω (T.E. system Z = 50 Ω). Investigation of such amplifiers is planned for the near future.

If the full potential of an NF-meter optimised preamplifier is to be utilised in practice, then matching to the antenna is unavoidable.

These experiments have shown that a line-length of $\lambda/2$ (or multiple) between antenna and preamplifier presents the latter impedance, without alteration, to the antenna terminals. An optimum noise match between antenna and amplifier is, on account of this, only possible by the introduction of an adjustable (by a $\lambda/4$ at least) line-stretcher.

The total stretch from the antenna terminals, including where fitted, coaxial relays and the line-stretcher, can be adjusted for optimum signal-noise ratio by means of solar-noise or a signal from a weak transponder.

References

1) UHF-Unterlage DJ 9 HO
2) Radio Communication April 1982

Joachim Kestler, DK 1 OF

PLL-Oscillators with Delay-Lines Part 4: Carrier Noise Sidebands

6. MEASURING CARRIER NOISE SIDEBANDS

If the carrier noise sideband test results of the high frequency VFO (3) and also the data of the Braun SE-401 (fig. 3 in (1)) are considered, the impression may be gained that the noise characteristics of PLL/DL oscillators are mainly of mediocre quality. This however, is not the case, much more to the point is, that the characteristics of the oscillator tuned-circuit itself are of decisive importance and comparitively, the above cited specimens of this type are not exactly shining examples. The VFO described in (3) may have the fault of a relatively tight coupling of tuning-diode to the tuned-circuit but this is unavoidable in view of the wide tuning range (+ 10 %) required.

How the carrier noise of the oscillator affects the receiver characteristics has been extensively shown by DJ 7 VY in (1). The measurement technique will be considered in this article followed by noise data determined from a specimen 2 m oscillator constructed from DK 1 OF 046/047.

6. 1.Measurement Technique

To get it quickly out of the way, a "normal" spectrum-analyser (price group DM 80.000) is not much use here because the instrument's local oscillator noise masks the noise of the test-item owing to its multi-order tuning range. Also, the best dynamic range of 80 dB, offered by such instruments, is too small. Modern FFT (fast fourier transform) analysers are only suitable for relatively low frequencies since the signal under test must be digitalised with an adequate resolution (e. g. 16 bit) before the computer is able to compute all components of the signal's spectrum in the given time-frame.

It is expedient to translate the frequency to be examined, by means of a mixer and an extremely low noise local oscillator, down to a lower frequency where it may be observed more simply. This "intermediate frequency" can also be zero i. e. the same frequency L. O. as that of the test-signal thus enabling the use of a small AF filter to select the noise sideband before rectification (RMS) and display.
Any other IF can, of course, be employed if the necessary steep-flank filters with sufficient stopband attenuation are available. This concept, as in **fig. 33**, will be examined more closely. The reference oscillator used was that by DK 1 AG (circuit diagram fig. 10 in (4)) together with the following crystal filter shown in fig. 20 (4). Following the buffer stage, a high-current FET, the 72,5 MHz crystal signal is frequency doubled and amplified to a power of 200 mW by two hybrid amplifiers (Avantek UTO-546). The mixer is a super-high level type, which can take a 23 dBm LO injection power, giving a 1 dB compression at a signal input of 20 dBm.

The VHF oscillator under test is amplified by a further hybrid amplifier to 10 mW and fed via a calibrated attenuator (x 2 cascaded, Weinschel

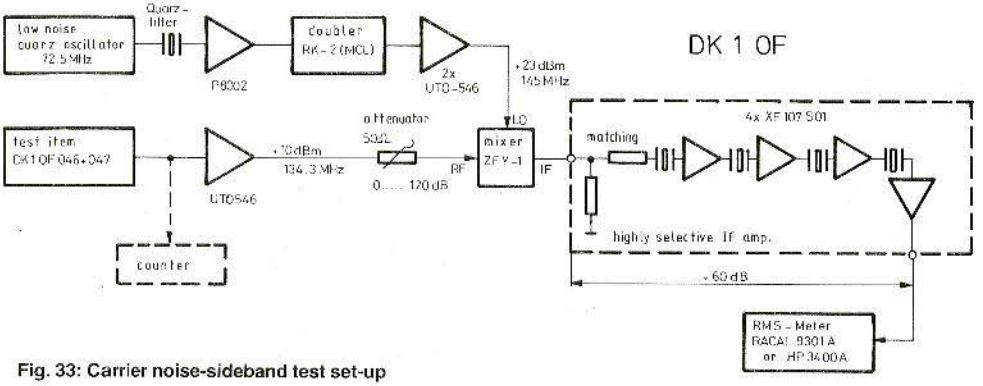

Fig. 33: Carrier noise-sideband test set-up

Typ 3023) to the mixer RF input. The resulting 10,7 MHz IF frequency is then selected by a highly selective IF amplifier using industrial-surplus crystal filters (XF 107 S 01 by KVG) together with a very steep flank, 32 pole filter, also obtained cheaply (there's some more left). Owing to the cascaded filters, the pass-band ripple (4 dB) makes an exact determination of the noise-bandwidth necessary. This was carried out by graphical integration on a linear format and resulted in a noise-bandwidth of 6,1 kHz. A signal, 5 kHz from the mid-band frequency, is attenuated by more than 130 dB. The output of the IF amplifier is connected to an RMS-voltmeter (Racal 9301 A).

Now for the carrying-out of the measurements. First of all, the VHF oscillator is adjusted to a frequency of exactly 134.3 MHz in order that a signal of 10.7 MHz appears in the IF. The attenuator is adjusted for say 10 mV RMS in the output meter and its setting noted (ensure that the IF stage is not limited by noise nor saturated by signal). The VFO is now tuned say 10 kHz off frequency, with the aid of a counter, and the attenuator readjusted in order to return to the 10 mV reference in the output meter. This reading is the result of carrier noise-sidebands. The attenuator setting is again noted.

Example:

VFO at centre-band: a = 112 dB for reference of 10 mV (RMS)

VFO tuned 10 kHz high: a = 8 dB for reference of 10 mV (RMS)

Carrier to noise C/N = 112 − 8 = 103 dB in 6 kHz noise slot

BW shrinkage factor for 1 Hz slot = 10 log (6 x 10^3/1 Hz) = 38 dB

C:N at 10 kHz from carrier = 103 + 38 = 141 dB in 1 Hz slot

in other words: C:N = 141 dBc, 10 kHz from carrier

Noise signals are characteristed by a very high crest-factor (peak to RMS ratio). This means a noise power (or noise voltage) measuring instrument must have a sufficiently high dynamic range in order to hold measurement errors within reasonable bounds. The instrument should have a crestfactor of at least 40 dB requiring that a reference set at 10 mV RMS calls the instrument to handle 1 V undistorted (on the range)
note: HP 3400 A has a crest-factor of 10 dB at FSD and 40 dB at 10 % FSD.

Should further information upon noise measurements be required the reader is recommended to references (5) and (6).

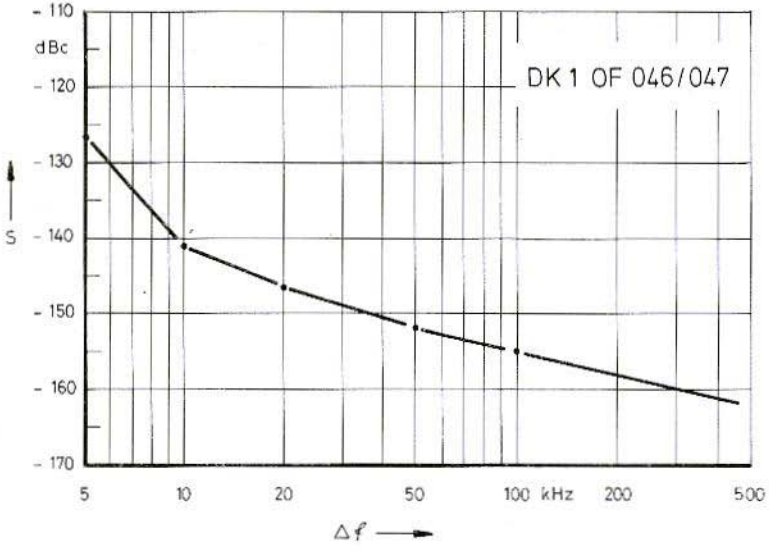

6.2. Test Results

The noise spectrum of the VHF oscillator DK 1 OF 046/047 is represented in **fig. 34.** A comparison with the original version (1) indicates good agreement. The curve of course, shows both noise from the test-item and also from the instrument's **(fig.33)** local oscillator.

The construction article announced earlier which will deal with a suitable receiver input stage has had regrettably, to be delayed somewhat owing to the intensive work for the above article.

References

(1) Martin M.: Low noise VHF-Oscillator with Diode Tuning
VHF Comm. Vol. 13, 2/1981, P. 66-82

(2) Kestler J.: PLL-Oscillators with Delay-Lines Part 1
VHF Comm. Vol. 16, 4/1984, P 211-220

(3) Kestler J.: PLL-Oscillators with Delay-Lines Part 2
VHF Comm. Vol. 17, 1/1985, P 46-54

(4) Neubig B.: An extremely Low-Noise 96 MHz Crystal Oscillator. Part 2
VHF Comm. Vol.13, 4/1981, P 194-203

(5) Neubig B.: An extremely Low-Noise 96 MHz Crystal Oscillator. Part.1
VHF Comm. Vol.13, 3/1981, P. 135-143

(6) Scherer D.: The "Art" of Phase Noise Measurements
Hewlett-Packard May 1983

(7) Kestler J.: PLL-Oscillators with Delay-Lines. Part 3
VHF Comm. Vol. 17, 2/1985, P. 112-120

Horst Burfeindt, DC 9 XG

GaAs-FET Inter-Locked Dual-Polarity Power Supplies for portable Use

This supply is suitable for use with two-stage GaAs-FET amplifiers in the higher GHz range. It features a protection circuit which prevents the drain voltage V_D from being applied without the gate voltage V_G. The PCB contains also a DC to OC converter which doubles the battery voltage from 12,6 V to 24 V without the use of a transformer. This voltage serves to supply the coaxial relays (surplus Y type) which require 20 to 28 V.

1. CIRCUIT DIAGRAM

The drain voltage supply (**Fig. 1**) is undertaken by an LM 723 stabilizer in a 14 pin DIL format. The

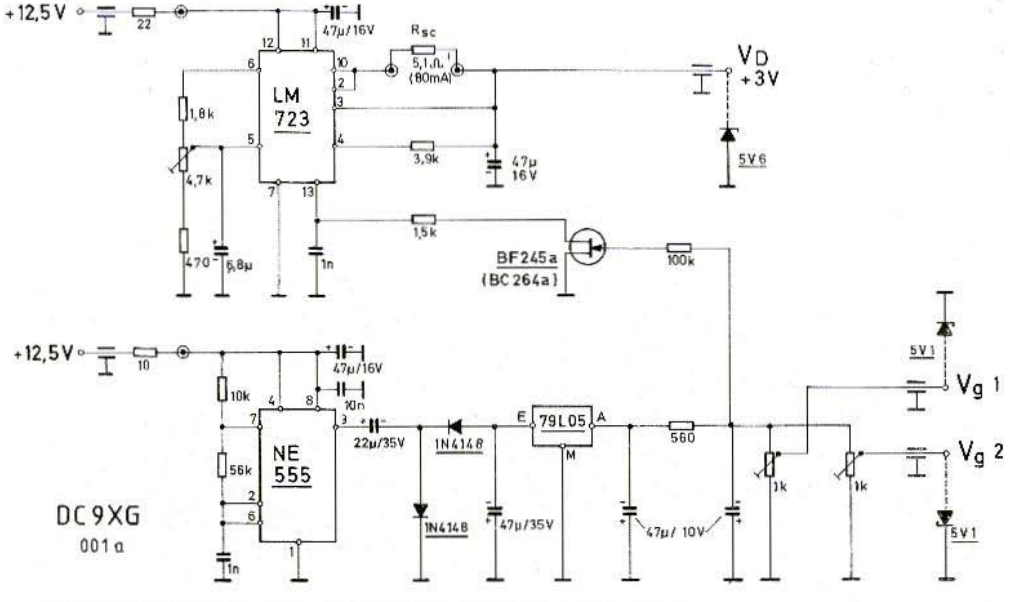

Fig. 1: GaAs-FET supply with current limiting and fail-safe interconnection

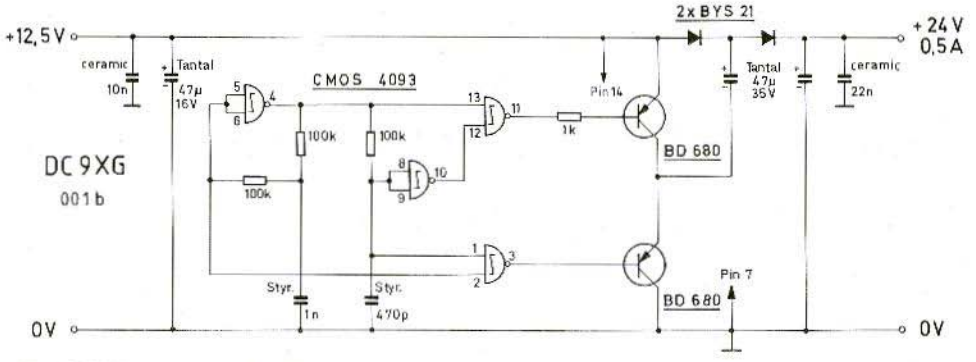

Fig. 2: DC Voltage-doubler 12/24 V at 0,5 A

output voltage is adjustable, with the 4,7 kΩ preset, to between 1 - 5,5 V. The resistor R_{SC} limits the current and is calculated from the formula:

$$I_{max} = 0.45\ (V)/R_{SC}(\Omega)$$

A resistance of 5,1 Ω limits the current to approx. 85 mA.

The gate voltage is produced by means of the well known timer NE 555 connected as a multivibrator followed by a voltage-doubler. The voltage regulator 79L05 stabilizes the negative voltage at -5 V. A 560 Ω resistor at the output serves as a filter and at the same time, as a part of a voltage divider together with the 1 kΩ presets. The complete filter, comprising 560 Ω/47 µF elements, suppresses the internal noise of the 79L05.

1.1. Gate-/Drain Supply Interconnect

The divided negative voltage at the top of the two 1 kΩ presets is −2,35 V. This negative voltage biases the field-effect transistor to cut-off. This FET conducts at zero gate potential and effective-

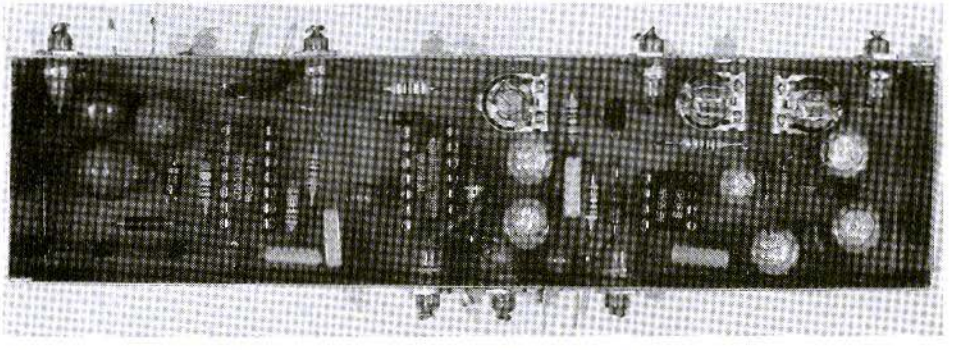

Fig. 3: Prototype module showing all external connections taken via feedthrough filters

ly returns pin 13 of the LM 723 to earth via the 1,5 kΩ resistor. This controls the LM 723, making the internal series pass transistor non-conducting and the output drain voltage near zero.

The purpose of this arrangement, is to delay the drain voltage until the presence of the negative gate potential has been assured. Should the gate bias supply fail altogether, then the drain supply is also nullified.

It is important that the transistors used for this purpose are N channel FET's with the A suffix, e.g. BF 245 A/244 A (TI) or BC 264 A (Valvo). Only

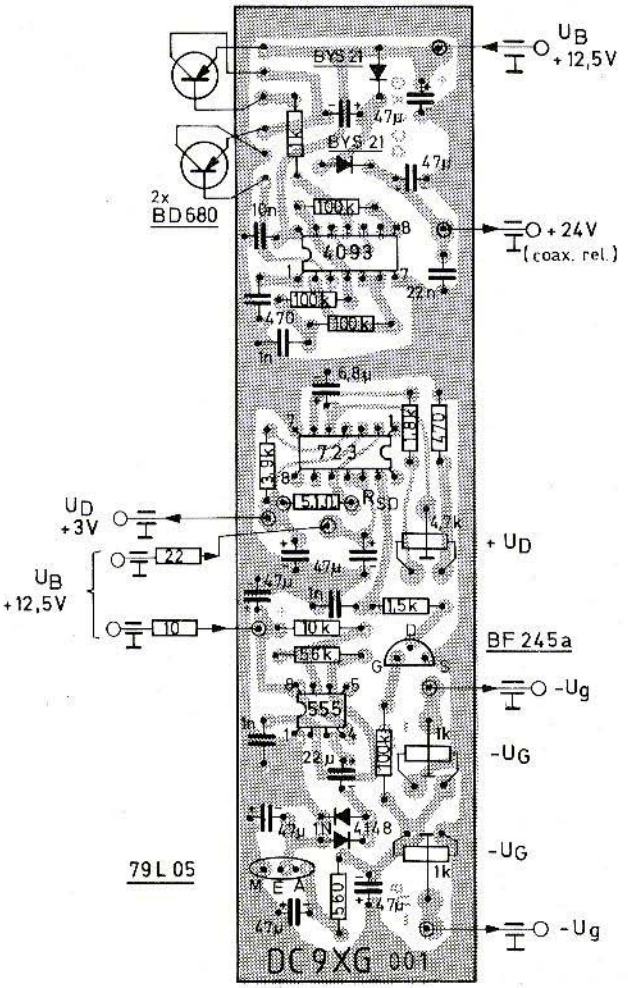

Fig. 4:
Component plan of PCB DC9XG 001 showing external connections. Pins 1 and 8 of 4093 must be connected by a wire bridge on track side of board

these types of transistor cut-off at −2 V gate potential. The B version of the BF 245 requires a V_G of -3,5 V to cut it off.

2. DC VOLTAGE-DOUBLER 12/24 V

The converter in **Fig. 2** supplies the author's two parallel connected 28 V SMA coaxial relays at a total supply current of 0,5 A.

2.1. Circuit Diagram

In order to obtain the correctly phased control for the two PNP Darlington-transistors BD 680, an oscillator comprising 4 C-MOS Schmitt-triggers, encapsulated in one chip RCA "4093", is used. Low resistance LOC-MOS types cannot be used here as the transistors draw too much quiescent

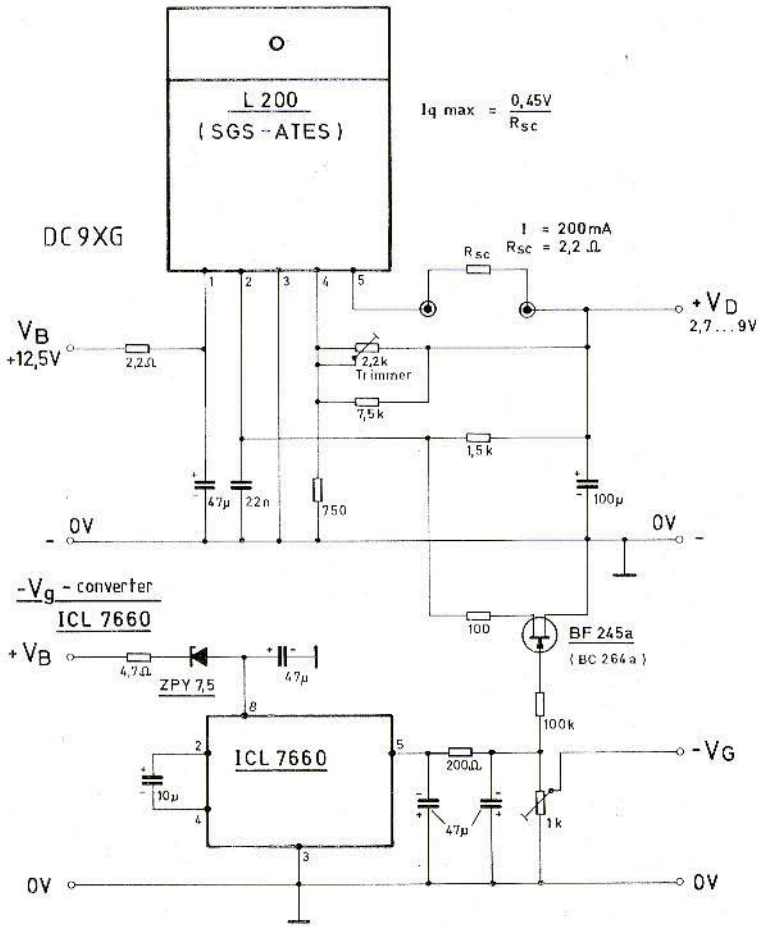

Fig. 5: Suggested circuit for Power GaAs-FET Supply

current, become hot and do not switch reliably. The oscillator frequency is 11 kHz and is rectified by a Schottky 1 A power-diode. On account of high frequency, tantalum electrolytics are used for the blocking and reservoir capacitors.

2.2. Data

VB = 12,5 V
Quiescent current = 7 mA
Converter frequency = 11 kHz
Output voltage = 22 V at R_L = 100 Ω, I_B = 430 mA
Output voltage = 24 V at V_B = 13,8 V, R_L = 68 Ω, I_B = 700 mA

3. CONSTRUCTION NOTES

The GaAs-FET supply and voltage-doubler is housed in a standard tin-plate box 37 x 148 mm (**Fig. 3**). The unit has been working now for two years in the author's 9, 6 and 3 cm band equipment.

The unit can be used as a test-bench supply for GaAs-FET experiments by replacing the current limiting resistor and preset variables controlling $+V_D$ and $-V_G$ for continuously-variable potentiometers mounted on a front panel.

The single-sided PCB DC9XG 001 (35 x 145 mm) is shown in **Fig. 4** together with component layout. The two ICs LM 723 and NE 555 are supplied via 22 Ω and 10 Ω resistors respectively, by 12,5 V.

The series resistors are necessary in order that the send/receive relay does not stick closed owing to the 47 µF capacitors across the 12,5 V supply.

The protection zeners, shown dotted in **Fig. 1**, are actually located on the preamplifier PCB. These diodes should always have a zener voltage which is above 4,7 V. Z-diodes having a zener voltage below 5,1 V do not have a steep characteristic and a current could flow at voltages around 3 V.

4. POWER GaAs-FET SUPPLY

Figure 5 shows a suggested circuit for a power GaAs-FET supply. The drain voltage is stabilized with an SGS-ATES L200. The output voltage is variable between 2,7 and 9 V. The maximal current is 2 A and may be dimensioned by choice of the resistor R_{SC} according to the following formula:

$$I_{max} \approx 0{,}45\ (V)/R_{SC}(\Omega)$$

The converter for the negative gate bias uses the monolithic C-MOS converter ICL 7660 CPA (Intersil).

The $-V_G/+V_D$ interlock transistor is again the J-FET type BF 245 A. A zener-diode ZPY 7,5 V, in series with V_B, reduces the heat-loss of the converter chip, thereby preventing latch-up.

The filter network at the output of the ICL 7660 suppresses the converter switching frequency signal.

The L200 can, of course, be combined with an NE 555 as a converter for a negative supply.

Jochen Jirmann, DB 1 NV

A Stable Crystal-Controlled-Source for 10,37 GHz

Two families of equipment have evolved for the 3 cm band, the simple, unstabilised Gunn or FET oscillators for portable, wide-band, FM equipment and complex quartz-stabilised systems for fixed-station SSB. Unfortunately many people have considerable anxieties about varactor multipliers which tends to explain the dearth of usable construction articles about them (such as the X9 multiplier by DK2VF/DJ1CR).

This article describes a simple-to-construct oscillator chain which delivers more than 10 mW at 10,37 GHz without using complex milled and rotary parts.

1. THE CONCEPTION

The author has constructed two well-known modules, the 1152 MHz multiplier (DCØDA) (1) and the X9 multiplier DK2VF/DJ1CR (2) and with some important improvements has developed a simple and reliable concept. The block-diagram is shown in **fig. 1** which represents the two units together.

2. THE 1152 MHz GENERATION

The 1152 MHz multiplier chain is almost exactly identical with that of the DCØDA 005 module, except the following modifications were carried out: –

- an FM modulator was included as an integral part of the crystal oscillator,
- the discretly-built voltage regulator was replaced by a 78LØ8,
- instead of the simple λ/2 circuit at the module's output, a three stage, micro-strip filter has been included which ensures a 50 dB suppression of spurs and harmonics,

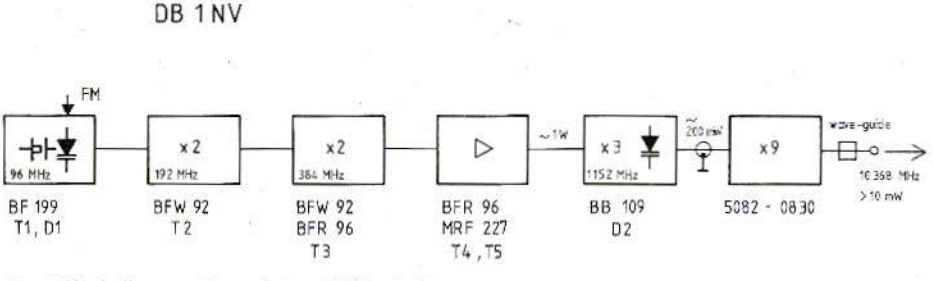

Fig. 1: Block diagram of complete multiplier chain

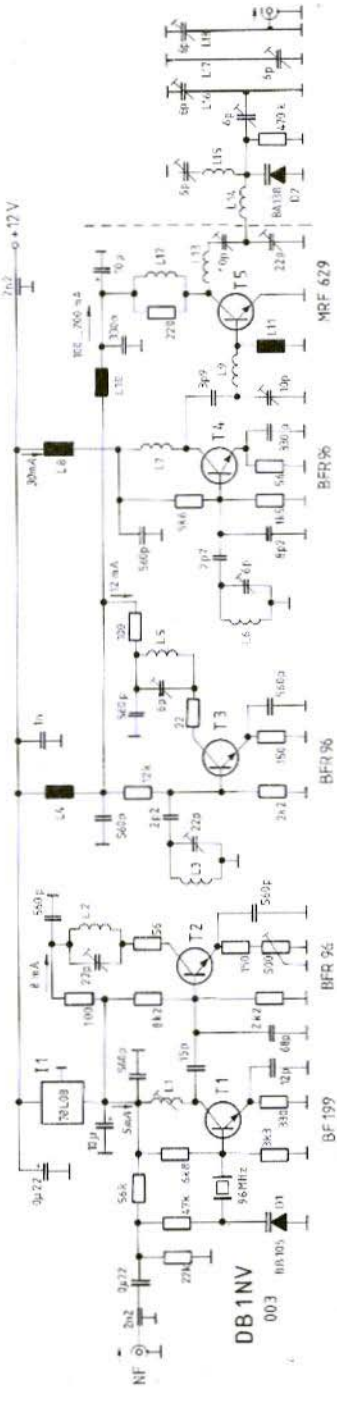

- easily obtainable, Valvo foil-trimmers were used exclusively throughout,
- all stages are built according to the recommendations of DJ1ZB and are sure-fire and easy to tune,
- the output power can be adjusted by one trimmer
- the PCB could be reduced to 70 mm x 145 mm thereby fitting into a standard tin-plate container.

Figures 2 and 3 show the circuit diagram , the PCB layout, and the component placement of the PCB DB1NV 003.

2.1. Components for the PCB DB1NV 003

Semi-conductors

T1 :	BF 199, BF 224 or equiv. BEC series
T2, T3:	BFW 92, BFR 96 (T-plastic case)
T4:	BFR 96, BFT 12 (T-plastic case)
T5:	MRF 227, MRF 629 (T039 with **emitter** to case)
D1:	BB 105, BB 505
D2:	BB 109, BA 138 or if need be, BB 105 or BB 505
IC1:	78L08 voltage regulator

All trimmer-caps: Valvo foil 7,5 dia
All capacitors: ceramic 5 mm lead spacing
All electrolytics: Tantalum
Resistors: 0207 construction

Winding details

L1:	5,5 turns, 0,3 CuL on 4 mm form with UHF core
L2, L3:	1,5 turns, internal dia 7,5 mm
L4:	1 µH choke
L5, L6:	wire loop 6 mm internal dia, 12 mm hole spacing
L7:	10 turns, 0,5 mm CuL, internal dia, 3 mm

Fig. 2: Circuit schematic of the 1152 MHz generator

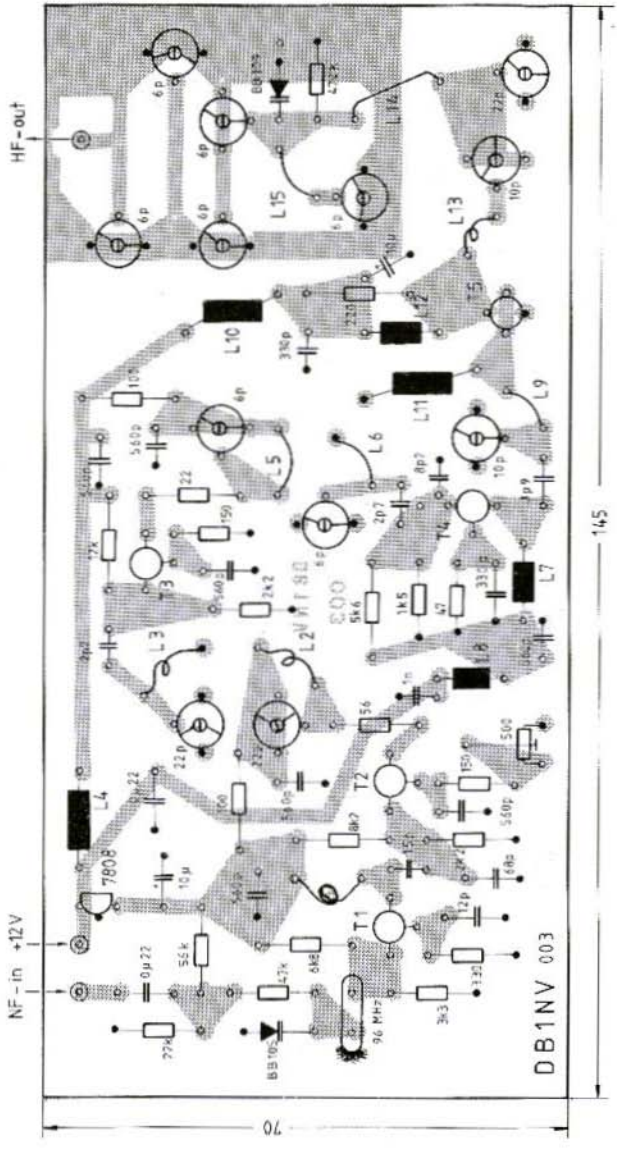

Fig. 3:
Component layout of 1152 MHz generator (• soldered to ground on upper-side of PCB)

L8:	1 µH choke	L13:	1,5 turns, internal dia, 6 mm
L9:	wire loop 6 mm internal dia, 9 mm high	L14:	1,25 turns, internal dia, 6 mm
L10, L11:	Broadband choke VK 200	L15:	2 turns, internal dia, 2,5 mm
L12:	10 turns 0,5 mm CuL, internal die 3 mm	L16 - L18:	Microstrip-lines
		wire:	1 mm dia silvered

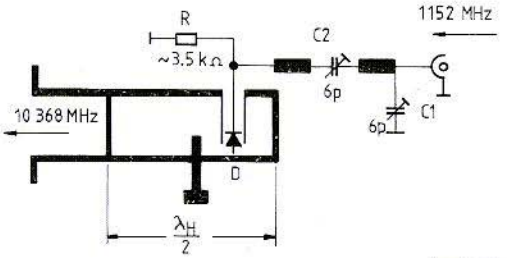

Fig. 4:
Electrical representation of the X9 multiplier

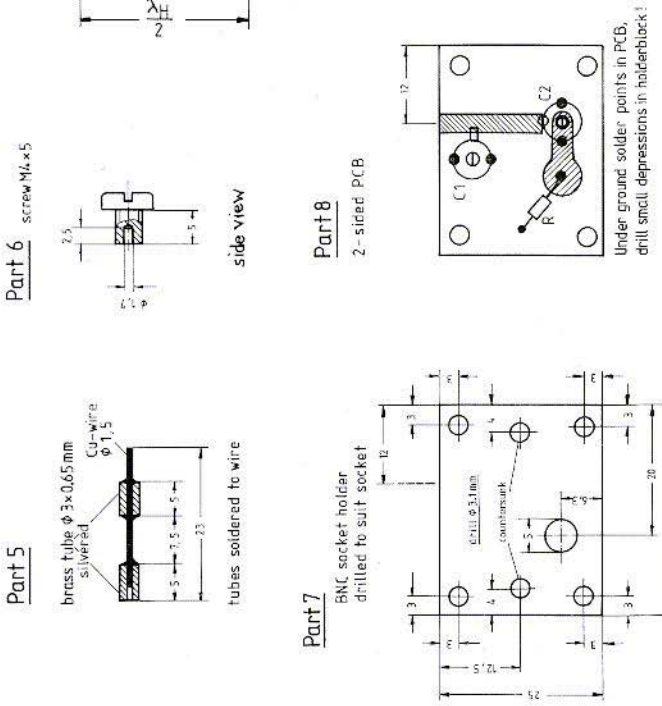

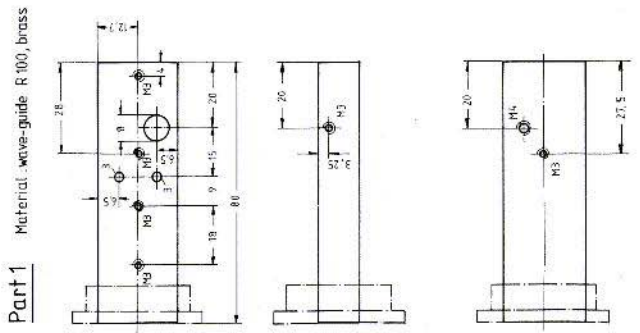

Fig. 5:
Component parts of the SRD multiplier 1152/10368 MHz
Part 2: wave-guide flange R 100
Part 3: short-circuit slider brass 22,7 x 10 x 10 mm to fit in W/G
Part 4: λ/2 line, Brass tube, 5 dia x 0,5, 18,5 mm long
Part 9: brass posts 12,7 mm x 3 mm dia

As can be seen, the circuit exhibits no particular features, only the selection of the varactor represents a little trial and error. The author found that the BA 138 (no longer manufactured) and the BB 109 proved successful. Even some 1N4148 diodes could be used, following adjustment of the working point by a suitable parallel resistor.

2.2. Construction Notes

Those, who are not afraid of a little metal-work can construct the output filter from lines and trimmers supported above the PCB plane, thereby obtaining somewhat more output power. The correct tune-up procedure for a multiplier has been dealt with so often that it will not be repeated here in detail. A diode probe with an indicator will be useful to adjust each stage, in turn, for maximum output when coupled to its tuned circuit. The output should be a little over 200 mW for the microstrip version and 300 to 400 mW for the air-dielectric version.

3. THE X9 MULTIPLIER

An SRD (step recovery diode) HP 5082-0830 is employed in order to multiply the frequency from 1152 MHz to the final frequency of 10368 MHz. This diode is considerably cheaper than the earlier type recommended by DJ1CR but has a somewhat lower efficiency. Whereas DJ1CR obtained efficiencies in the order of 10 to 15 %, the circuit recommended here works with only 5 to 10 % according to the diode selection. Diodes possessing a higher breakdown voltage tend to deliver more power.

As **fig. 4** shows, the multiplier comprises a matching circuit for 1152 MHz, the diode itself, as well as a half-wave, short-circuited line associated with the diode. The half-wave section oscillates at a greatly reduced attenuation at the final frequency in accordance whith the current impulses through the diode. The required final frequency is then selected by a post-coupled wave-guide resonator.

More information about SRD multipliers can be found in the Hewlett-Packard Application Notes 918 and 920. **Fig. 5** shows the component parts of the multiplier. The following materials are required: R 100 wave-guide, brass-plate 25 mm x 10 mm and 3 mm dia. external, 1,7 mm dia. internal, as well as 5 mm external, 4 mm internal, diameter brass tubing. The brass tubing may be obtained from model hobby shops.

3.1. Construction

First of all, the wave-guide section, part 1 in **fig. 5** (preferably made of copper owing to its high heat conductivity), is suitably drilled to receive the diode holder. The holding block 7 is also drilled and prepared for the matching circuit. After a test assembly according to **fig. 6** the drilling for the diode-holder is checked to see that it is in alignment with the W/G hole. The brass M 3 holding screws for the diode-block are filed down flush with the inner surface of the wave-guide. The two 3 mm dia. posts (part 9) of the filter are placed in the wave-guide, the wave-guide flange (2) is placed over the end and the whole assembly soldered together. The $\lambda/2$ line (part 4) is soldered into the brass block. The choke (part 5) is constructed as shown in **fig. 5** by slipping the two 5 mm long, 3 mm dia. tubes over a 23 mm length of silvered 1,5 mm dia. wire. The tubes are placed in position and soldered, the whole choke assembly insulated with teflon tape. The sliding short-circuit (part 3) is provided with 0,1 mm copper foil surfaces to slide on, thus making a better binding contact with the inner wave-guide surfaces without a precision mating being necessary.

The tuning-screw on the side wave-guide wall, forms a capacitance for the $\lambda/2$ section and is tuned for best results – it is sometimes not necessary.

Before mounting the matching components on the PCB, the brass block (7) must be suitably drilled to provide sufficient clearance for the solder points on the underside of the PCB. The PCB must lie on the brass block according to the component layout.

After the assembly has been completed, the diode is inserted by ensuring that the heat-sink

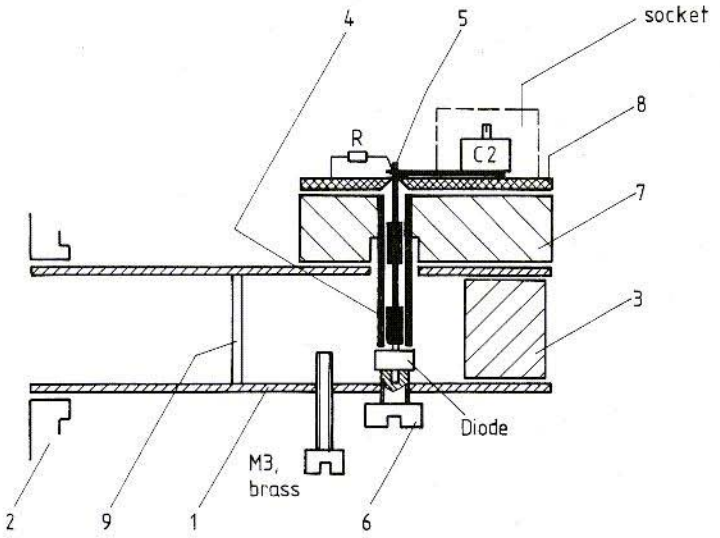

Fig. 6: cross section of X9 multiplier

end (without ring) is placed in the screw-cap (part 6) thus using the greater mass of the wave-guide to dissipate the heat. Use also a little heat contact paste for this purpose. **Fig. 7** shows the completed multiplier.

3.2. Tuning

The tuning of an SRD multiplier is not exactly easy but the diodes are so robust that they cannot be damaged during tuning. A good indication of the correct tune point is, that when the tuning elements are turned, the power varies smoothly and without sudden jumps. A signal-generator adjusted to 1152 MHz and 200 to 300 mW output power is applied to the BNC input socket. This bias potentiometer is set to 3 or 4 kΩ and the input trimmer adjusted for maximum voltage across the diode. The output circuit is then adjusted for maximum output power. The short-circuit slider is about 5 to 7 mm behind the diode. **All** elements are then tuned in order to maximise the output power by a **process of iteration**, as the position of some controls may be mutually dependent. The input power from the generator is then increased to 600 mW when the output power should saturate at 30 to 40 mW.

The preset potentiometer may be replaced by a fixed resistor if desired. This turned out to be 3,5 kΩ on the prototype and a standard 3,3 kΩ resistor was used to fix the diode working point. This, however, is temperature dependent and it may have to be determined again later. Suitable circuits for this may be found in HP application notes 918 and 920.

4. TESTING

The complete multiplier chain was fed into a cavity mixer which had an IF amplifier DB1NV 001 (3) connected to its output port. The assembly formed a simple FM receiver. The output power was adjusted for maximum receiver sensitivity which occured at 10 mW, the noise figure being 9 dB. Test contacts with DG2ND confirmed the usability of the system.

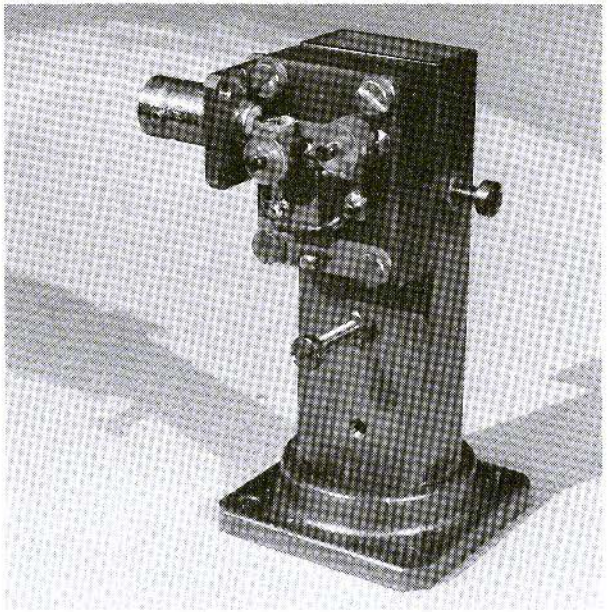

Fig. 7:
X9 multiplier prototype

5. REFINEMENT POSSIBILITIES

For stationary use, the simple crystal oscillator can be replaced with a low-noise FET in a temperature-controlled oven. For portable use, an oscillator, able to be pulled to allow a swing in output frequency of 3 MHz, may be useful. For this purpose, a 96 MHz crystal, in an external circuit, may be excited at its basic frequency (for greatest frequency pull) and then multiplied by 5 and fed into the existing crystal oscillator stage which then works as a buffer. The 96 MHz signal from the X5 multiplier must be inspected, however, for spectral purity.

The 1152 MHz generator can, of course, be used as a low-power transmitter for the 23 cm band but the author has not conducted any experiments with this possibility.

6. REFERENCES

(1) Dahms, J.:
A local Oscillator Module for 200 mW at 1152 MHz
VHF COMMUNICATIONS Vol. 10, Ed. 1/78 P. 18 - 22

(2) Griek, R. and Münich, M.:
A Frequency Multiplier for Narrow Band, 3 cm Band Communications.
VHF COMMUNICATIONS Vol. 11, Ed. 2/79 P. 66 - 73

(3) Jirmann, J.:
A FM Transceiver for 10 GHz with dielectrically-stabilized Oscillator
VHF COMMUNICATIONS Vol. 16, Ed. 1/84 P. 2 - 12

Erich Stadler, DG 7 GK

Measurement of Cable-Impedance with Impulses and Sine-Waves

Cables have the property, that impulses arriving at the cable-end are reflected to an extent which is dependent upon the degree of mismatch of load to cable characteristic impedance. The actual shape of the applied impulse waveform is of smaller importance. Because sine-waves may be regarded as both positive and negative impulses, they can also be used for measurement purposes. A condition of the measurement is, however, that the terminating impedance is purely resistive. The only value of terminating impedance which absorbs the impulse completely is that which is equal to the characteristic impedance Zo. Using sine-waves the reflection standing waves are caused to become unity and disappear using a swept display (wobbulator). This method is relatively fast.

1. USING IMPULSES TO MEASURE COAXIAL CABLE Zo

1.1. Test set-up

For this method, an oscilloscope and a pulse generator are required. The oscilloscope monitors the impulses which are transmitted down the cable **(see fig. 1)**. Not only the incident pulses are displayed, the reflected ones too are present. For a proper display, however, the time-base of the oscilloscope must be suitably adjusted as will be discussed later.

1.2. Method of measurement

Before the actual measurement can proceed, it must be ascertained that reflections are in fact present on the trace. The generator delivers a train of pulses which is displayed on the screen. On a short, low-loss length of cable the incident impulse has the same amplitude as the reflected impulse under unterminated conditions. In order that both may be identified, the far end of the cable is temporarily short-circuited. The reflected impulses will there-upon change their polarity.

The behaviour of the reflected impulses must be observed throughout the measurement process.

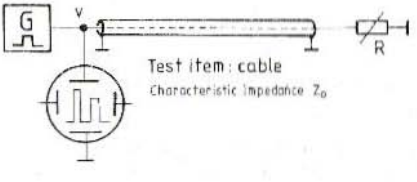

Fig. 1: Test set-up for Zo measurement using impulses

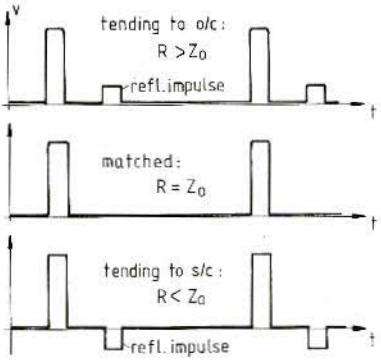

Fig. 2: Oscilloscope traces for various cable terminations

A known resistance R, which is estimated to approximate the characteristic impedance Zo, is used to terminate the far end of the cable. The amplitude of the displayed pulses will then become much smaller. If the reflected pulses tend to approach the amplitude of the incident pulses then it is clear that R is greater than the cable Zo. If the reflected impulse has a reversed polarity, then R is smaller than Zo (**see fig. 2**). If the reflected pulse disappears altogether, the terminating resistor R is exactly equal to the characteristic impedance of the cable Zo (**fig. 2 middle**).

It may be expedient to terminate the cable-end with a variable non-inductive resistor and measure the value of resistance, which has caused the reflected impulses to disappear, using an ohm meter.

1.3. Observations on time-base and test-equipment

The measurement can only be expediously carried out if the reflected impulses can be adequately identified from the incident pulses. That is to say, when the transmitted impulses are narrow in relationship to the repetition time (small duty factor) and that the cable is long enough to allow sufficient time between the end of the incident pulse and the start of the reflected pulse so that they do not merge. The pulse repetition rate should not be unduly high but sufficient to allow a stable triggered trace. A repetition rate of 50 Hz should be suitable if the pulse-width is sufficiently narrow.

1.4. Example

The characteristic impedance of a 10 m long cable of velocity factor 0,66 is to be determined. What is (a) the separation time between incident and return pulses, (b) a suitable time-base, (c) a suitable pulse width.

Solution: The propagation time along the cable is $v = 0.66 \times 300 \times 10^6$ m/s $= 2 \times 10^8$ m/s. For a 10 m long cable, the transmission time is 10 m/2 x 10^8 m/s = 50 ns. The reflected energy has a total transit time of twice that of the incident i. e. 100 ns. For a reasonable display the time-base should therefore be set to maximum 0,1 μ s/cm and at least 10 ns/cm. The pulse-width of the measurement pulses should be small in relationship to the time between incident and reflected pulses, in this case less than 50 ns.

For a clean trace, the oscilloscope should also have a y-deflection frequency of 10 to 20 MHz in order to ensure short rise and fall times on the displayed pulses. The pulse period should be so chosen in order that there is a sufficient time interval between the trailing edge of a reflected pulse and the leading edge of the next incident pulse. In the example above, a pulse repetition frequency of 2 MHz, i.e. period of 0,5 μs, can be used. The test-item used for demonstration purposes, shown in **fig. 3**, has a length of 100 m and can be tested at a PRF of 100 kHz and an oscilloscope bandwidth of only 3 MHz is sufficient.

1.5. Test-Method Limitations

The pulse-width of the signal generator impulses need not be a limiting factor. With a little practice it is possible to use relatively broad test pulse-widths. The incident and reflected pulses overlap

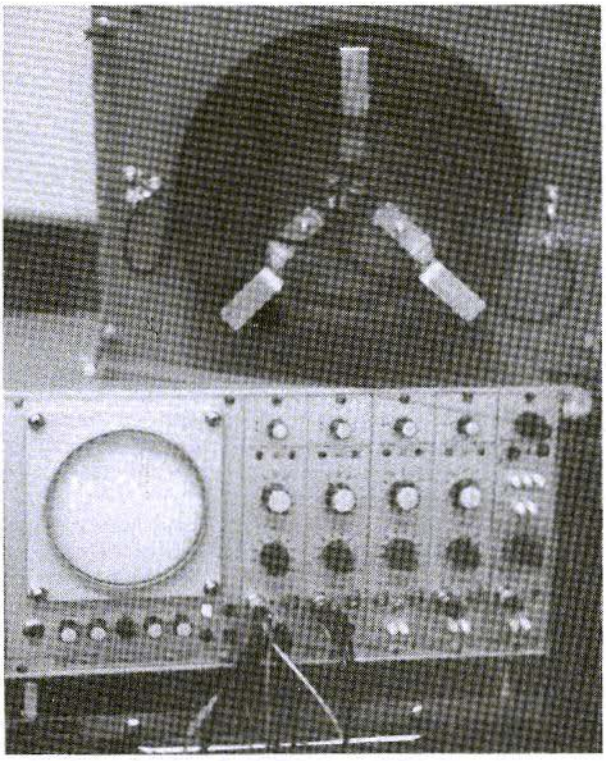

Fig. 3:
RG-58-Cable, length 100 m and monitored impulses
Photo: Electronic School Tettnang

and cause the incident pulse to be stepped in the manner shown in **fig. 4(a)**. A step-up is evident for a reflected pulse arising from a terminating resistor which has a higher value than that of the line's coaxial cable. In the same manner, reflected pulses from a lower terminating load than that of the cable impedance, cause a step-down (c) in the incident pulse. When the cable is terminated in its characteristic impedance the incident pulses are undistorted as shown in **fig. 4(b)**.

The test method is more severely affected by the limitation imposed by the oscilloscope **rise-time** and/or that of the pulse-generator used for the test. This makes it very difficult to see where one pulse ends and the other begins as shown in **fig. 5**. With regard to the required bandwidth of the oscilloscope and the minimum cable length

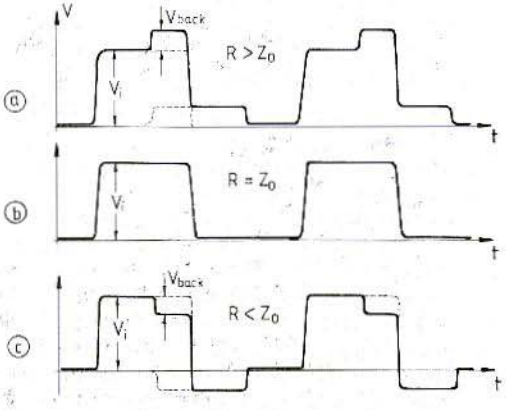

Fig. 4: Determination of Zo using "long" pulses

which is able to be tested, the considerations of the example indicate that the total rise-time should be less than 100 ns. Supposing that pulses from the pulse-generator had a 35 ns rise-time, the display oscilloscope should have a minimum bandwidth of: –

$$f_{BW} = 0{,}35/0{,}035\ \mu s = 10\ MHz$$

in order that the impulses are sufficiently faithfully reproduced on the trace. If cable lengths of under 10 m are required to be tested, then the oscilloscope bandwith would have to be increased and the pulse-generator would require a pulse rise-time of less than 35 ns.

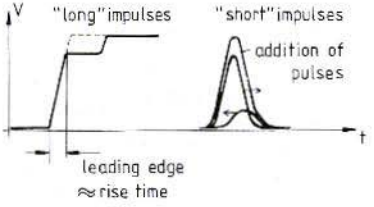

Fig. 5: Limitation of the reflection method owing to large pulse rise-time

2. USING SINE WAVES TO MEASURE COAXIAL Zo

2.1. Test-set-up

The equipment for this method differs from the measurement using pulses, as on the one hand a high-frequency signal generator is used and on the other hand the monitor is not an oscilloscope but a high-frequency probe with a DC meter as an indicator. The frequency of the generators should be variable over a very large range **(fig. 6)**.

2.2. Method of Measurement

First of all, the cable to be tested is either left open-circuit or short-circuited at the far and. Standing waves are set up along the length of the cable but they cannot be measured as the inner conductor is not accessable. If, however, the frequency is varied until say a maximum is indicated on the meter and then until a minimum is indicated, it will be apparent that the test may be carried out at one spot – the cable input end. It is only then necessary to note the difference between the indication at a voltage maximum to that at a voltage minimum. The bigger the difference, the bigger the mis-match. The measurement consists of varying the value of the load resistor until the difference between the maxima and the minima disappears to zero. The cable is then matched and the value of resistor for this condition represents the value of the cable's characteristic impedance Zo. As in the case of the pulse tests, the whole procedure is made less cumbersome by using a non-inductive variable resistor at the far end of the cable and measuring its resistance with an ohmmeter as soon as the voltage differential has been reduced to zero. The generator must have a constant voltage output over the range of the measurement. The signal generator could also be replaced by a wobbulator and the HF-probe and meter by an oscilloscope. Swept measurements are then made which simplify the measurement enormously. The load resistor is varied until the trace is flat, the cable is then matched **(fig. 6)**. The oscilloscope can be almost any

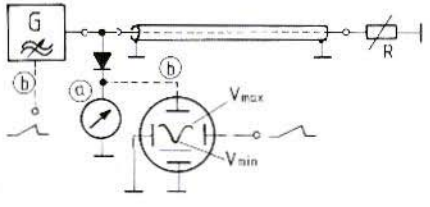

Fig. 6: Measurement of Zo using sine-waves
a) Manual frequency shift and meter indicator
b) Swept frequency and variations of voltage displayed on oscilloscope

available as no great demands are made upon it. It does not have to display high frequencies but merely the amplitude differences between the maxima and minima from the rectifier in the probe. When testing a long length of cable, the frequency difference between a voltage maximum and a voltage minimum need not be very large as will be seen in the following example.

2.3. Example

A 10 m long cable with a velocity factor of 0,66 exhibits a voltage node at the generator end when the far end is open-circuit. The generator frequency is 430 MHz which means that the number of wavelengths on the line falls short of an exact integer by $\lambda/4$. The frequency is raised to 435 MHz and exactly 22 wavelengths appear along the line and the voltage at both ends is maximum (anti-node). The frequency change to achieve this is 1,1 %. If this measurement was carried out, however, at say 100 MHz, the frequency change would have to be some 5 %. It would also be 5 % at 430 MHz, if the cable length was 2,5 m instead of 10 m.

2.4. Conclusion

Although the methods of determining a cable's characteristic impedance by pulses or sine-waves is efficacious, it is not the only method of measuring a cable's Zo. It may be done by measurement of L and C or by comparison of the exact amplitudes of incident and reflected waves thus obtaining the reflection coefficient. The latter will be the subject of another article.

Gerd Körner, DK 2 LR

The PCB - Integrated Coaxial Tuned Circuit

The methods introduced by this article should close the means of obtaining selectivity gap, which exists between stripline tuned circuits and cavity resonators, in the highest frequency range. The use of the "integrated coaxial circuit", devised by myself, should bring to many constructional projects a substantial simplification and also miniaturisation of circuits in the microwave area.

Since the principle is not limited to a certain frequency, it is left to the readers of this article to ascertain the limits of the technique. I have built test circuits working between 2 and 10 GHz. A preamplifier will serve as an example which according to the position of the tuning plunger will operate in the 12, 9 or 6 cm band.

1. THE PRINCIPLE

The low-noise, selective pre-amplifier mentioned above, is shown in **Fig. 1** as a mixture between circuit diagram and constructional sketch. For the 12 cm band the following data was determined, G > 10 dB, BW < 20 MHz, $F_{dB} \approx 2$ to 3 dB. This was attained with a drain current of 10 mA at which value, no current flowed in the zener diode protection device. The main items of interest are the two PCB integrated coaxial circuits. In order to understand their operation the current distribution in both, cylinder and in pot resonators, will be considered **(Fig. 2).**

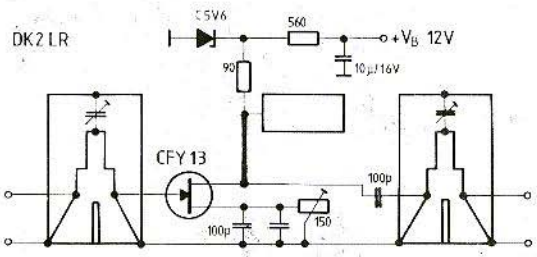

Fig. 1:
Low noise selective pre-amplifier for the 12, 9 or 6 cm band

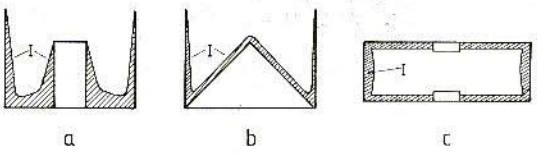

Fig. 2:
a) Highly non-uniform current distribution in an actual coaxial circuit
b) uniform current distribution in an ideal coaxial circuit
c) the current flow is greatest over the largest surface areas in the cavity resonator

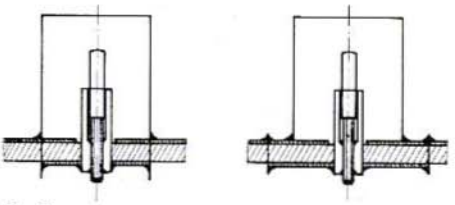

Fig. 3:
Side view of the PCB integrated coaxial tuned circuit
a) Shield recessed and inserted into PCB. The PCB ground plane does not contact along the slot inside the shield
b) Copper foil in slot, shield soldered onto PCB

The current distribution in the pot resonator shows clearly why it possesses a high circuit Q. The point is, the reduction of skin effect loss occasioned by the use of large, good conducting surfaces and the avoidance of lossy dielectrics (glass epoxy material) particularly at the "hot" end of the tuned circuit.

Strip-conductor tuned circuits must then, have a broad current distribution and at the "hot" capacitive end tapering-off or better still into air or some other high quality dielectric. With this, by the way, a further disadvantage of strip-line circuits is not yet remedied, namely the radiation of SHF energy from the PCB into space which represents a further loss.

At small wavelengths there is actually nothing against leaving the hot portion of a tuned-circuit off the PCB and putting it into coaxial form in a screened enclosure. In this manner, but at the cost of more mechanical effort, the integrated coaxial circuit was evolved thereby avoiding the aforementioned disadvantages of the strip-line tuned circuit.

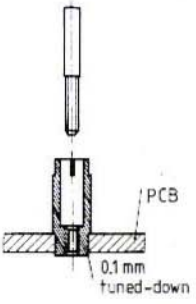

Fig. 5:
Mechanical principle of tuning plunger

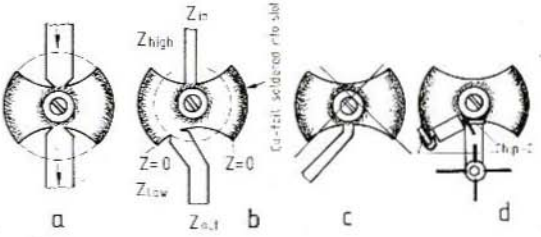

Fig. 4:
PCB integrated coaxial tuned circuit top view
a) PCB connecting lead without transformation
b) with step-down transformation

2. THE PRACTICAL CIRCUIT

As the **diagrams in 3 and 4** indicate, the surfaces carrying the greatest portion of the current in the tuned circuit are etched out in an exponential form on the PCB. The hot portion is mounted perpendicular to the etched PCB and consists of a coaxial arrangement of a 4 mm tuning plunger provided with a screw thread which runs through a 5 mm tapped bush all mounted in the centre of an 11 mm dia. shield. This arrangement opens up quite new possibilities as the PCB with these tuned circuits offers not only selectivity of the highest order but also a means of compensating reactive values. It is also possible to transform input and output impedance.

A connection to the PCB conductor at the foot of the plunger assembly represents a tap located near the cold end of the tuned circuit, which approaches the very low impedances of a transistor.

If a tap is required nearer the hot end of the tuned circuit, the PCB portion is simply made broader (but this increases dielectric losses) or a top capacity is added to the tuning plunger, thereby altering the circuits L/C ratio. The two "floor" pieces of the coaxial pot then having a greater share of the total circuit inductance. The SHF input and output connections are led-in at right angles to the leading edge of the floor-piece concerned, in accordance with **Fig. 4** (a and b correct, c incorrect). Supply voltage connections are taken to the circuit as shown in 4 d, i. e. parallel to the ground portion of the tuned circuit.

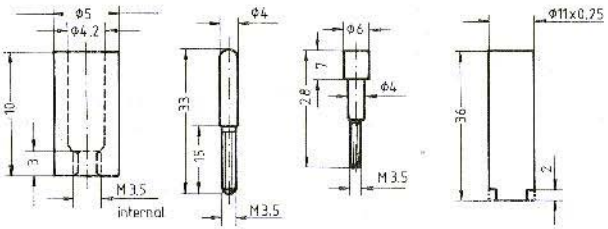

Fig. 6:
Components:
for the shield a piece of old telescopic antenna can be used. The length of the parts is given in Table 1

The mechanical principle of the tuning plunger is shown in **Fig. 5** whilst the dimensions of all parts are given in **Fig. 6.** The length of the tuning plunger is naturally, in accordance with the wavelength. **Table 1** contains the values for the three amateur bands.

Band	12 cm	9cm	6 cm
Plunger	33 mm	21 mm	12 mm
Bush	20 mm	20 mm	10 mm

Table 1

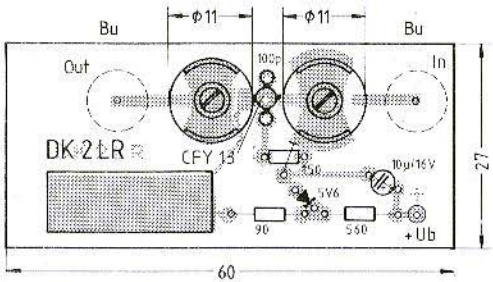

Fig. 7: PCB and component layout for the amplifier of Fig. 1

3. AN EXAMPLE

Now for the pre-amplifier mentioned in the introduction to this article, the PCB and component layout of which are shown in **Fig. 7**. The two-sided PCB is made from glass-epoxy and measures 60 x 27 mm. The use of this lossy material at SHF is made possible because the low impedance portions of the circuit remain on the PCB whereas the hot high impedance parts of the resonators are located in the integrated coaxial circuit in air. Also the separation of the other components can be kept to a minimum thanks to the non-radiating coaxial circuit.

Fig. 8 shows a gain/frequency curve as measured by DB 2 IZ. The frequency markers are 2120, 2320 (centre) and 2520 MHz. The 10 dB points have a bandwidth of 34 MHz. Finally a proposed method of sinking the source chip bypass capacitors into the PCB is shown in **Fig. 9.**

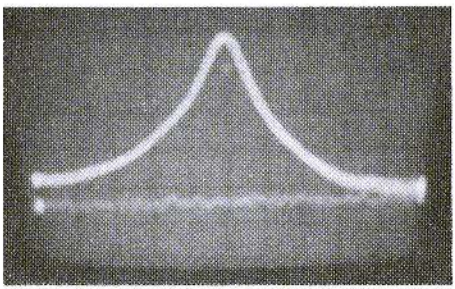

Fig. 8: Power gain/frequency characteristic of 13-cm-amplifier of Figs. 1 and 7
f_{mid} = 2320 MHz; BW_{-10dB} ≈ 34 MHz

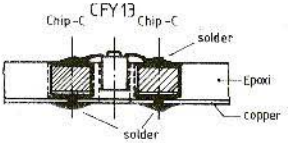

Fig. 9: Grounding of GaAs-FET source connections via chip capacitors set into the PCB

Jochen Jirmann, DB 1 NV

A 12-V-Mobile, Switched-Mode Power Supply (SMPS) Part 3 (Concluding)

3. POWER SUPPLY CONSTRUCTION

To begin with, **a warning.**

A large portion of the power-supply works at mains potential and the isolation is provided by a small ferrite transformer. For this reason only experienced constructors familiar with mains practice (and in particular, mains transformer winding) should attempt this project. He should also have available either a variable mains isolation transformer (not an auto-transformer) or a 0-300 VDC mains isolated power supply and he should have already constructed a high-power supply.

The anti-interference filter capacitors in particular, should be in good condition and bear official approval marks from the national safety regulatory authority concerned (e. g. VDE, BS, IEC). Do not use junk-box components.

The setting-up too, requires very careful use, and experience with an oscilloscope. Short-cut testing methods are definately not for this project.

3.1. Wound Components

It is best to start the construction with the transformer and choke.

The choke L 1 is the easiest to fabricate using a transformer-kit **(fig. 4)** SM 55 consisting of a laminated C-form core. The two winding apertures should be filled (leave a 1 or 2 mm air-gap) with CuL (enamelled copper wire) 0,7 mm dia and the winding ends terminated at the "correct" polarity. Pieces of 1,5 mm PCB or Paxolin can be used as spacers for the slots between core parts and the 1,5 mm air-gap. To prevent the choke from humming, the core-halves together with spacers and

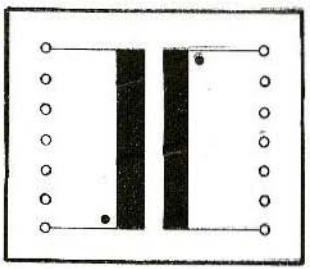

Fig. 4: Input choke L 1: Tnsfr. kit SM55 laminated core with twin coil bobbins. Both compartments filled (to within 1 – 2 mm) with 0,7 CuL windings. Air-gap: 1 mm.

coilbobbins, are assembled and glued with two-component adhesive and clamped in a vice.

The transformer construction is more complicated **(fig. 5)**. A bifilar winding consisting of a few metres of CuL (2 x 0,7 mm) is prepared for the primary n 1. About 21 turns are wound for the first single winding layer in order that it completely fills the bobbin length. Two layers of insulation are wound over this layer. The demagnetization winding n 2 is wound centrally over this with 50 turns of 0,5 mm CuL. Then another two layers of insulation followed by a further 21 bifilar windings of n 1. Again, two layers of insulation followed by the final 8 turns of n 1. In Juxtaposition to n 1, now wind 4 turns of 0,5 CuL for the auxiliary supply winding n 3. Over these two windings come four layers of insulation. Ensure that all the winding tails are fully insulated and terminated with the correct polarity indications **(see dots in fig. 5)**.

The secondary n 4 consists of ten 0,7 mm conductors twisted together which the author wrapped with teflon tape for extra insulation. The winding n 4 consists of 7 turns held in position by adhesive insulation tape, the ends are left flying but all ten conductors are cleared of enamel and soldered together.

A core-half can now be put in and held with a spring fastener. A few pieces of paper form an air-gap and the second core half is inserted and secured with the clip.

The choke L 2 consists of a core ETD 39 which has been wound with 15 turns of 10 x 0,7 mm twisted CuL. The air-gap should be 1 mm made from suitable insulation material.

The base choke consists of a 0,5 W/0,47 Ω metal-film resistor, upon which 12 turns of 0,5 mm CuL has been wound.

All the cores can be glued later, following testing, in order to prevent them from vibrating in sympathy with the SSB modulation thus causing a distorted audible sidetone.

If an adjustable high-voltage supply is available, the insulation between primary and secondary of the transformer should be tested at 5 kV - no discernable leakage-current should flow.

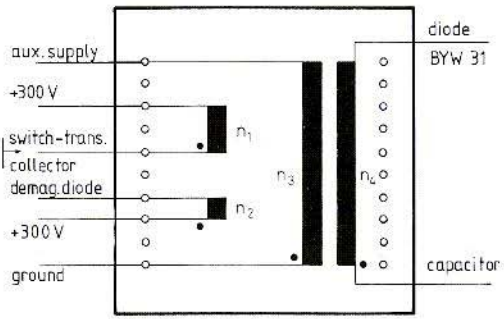

Fig. 5: Main Transformer T: Core ETD 49 with paper thichness air-gap
n 1: 50 turns 2 x 0,7 CuL parallel
n 2: 50 turns 0,5 CuL
n 3: 4 turns 0,5 CuL
n 4: 7 turns 10 x 0,7 CuL

3.1.1. Core Materials

Input Choke L 1: Laminated SM 55 with two-part winding bobbin and PCB mounting.

Power Transformer T: Core-kit ETD 49 (Valvo or Siemens) without air-gap and PCB mounting. Core material designation, Valvo 3C8, Siemens N 27.

Output Choke L 2: Core-kit ETD 39 (Valvo or Siemens) **either** without air-gap with suitable spacing material (0,5 to 1 mm) **or** core with 1 mm air-gap.

Output Interference Suppression Choke L 3, L4: Ferrite core 25 x 5 mm dia. each with 5 turns 2 - 2.5 mm CuL.

Core Material e.g.
Valvo tube core 4322 020 36810
or **rod core** 4322 020 39450
See para. 3.1. for winding details.

3.1.2. Winding Details

Input Choke L 1: Both compartments wound to

full capacity with 0,7 mm CuL (number of turns not critical)

Power Transformer T:

Primary n_1: 50 turns 2 x 0,7 mm CuL, first layer 21 turns, third layer 21 turns (demagnetising coil n_2 between) and 8 turns in fourth layer.
Demagnetising winding n_2: 50 turns 0,5 mm CuL
Auxiliary supply winding n_3: 4 turns 0.5 mm CuL in layer 4.
Mains insulation: 4 x transformer insulation foil.
Winding layer insulation: 2 x transformer insulation foil.
Secondary winding n_4: 7 turns 10 x 0.7 mm CuL (twisted)

Output Choke L 2: 15 turns 10 x 0,7 CuL (twisted)

Output interference suppressor choke: 5 turns 2 mm CuL
The winding diagrams are shown in **figs. 4 and 5.**

3.2. Other Components

Semi Conductors

T 1: MJ 16010 (Motorola) or similar **fast** bipolars with $V_{CEV} = 850$ V, $I_C \geq 5$ A, $B \geq 10$ or Power FET BUZ 54 (Siemens) or others with $V_{DS} \geq 850$ V, $I_D \geq 5$ A.
T 2: 2N2219 (fast switcher) or equivalent
T 3: 2N2905 (fast switcher) or equivalent
T 4: BF459 ($V_{CE} = 300$ V, $I_C = 50$ mA)
T 5, T 9: BC547 or equivalent
T 6, T 7,
T 10, T 11: BC557 or equivalent
1 Bridge rectifier 250 V(500 V), 1,8 A: B250 C 1800
3 fast diodes 800 V/0,4 A, BA 159 or equivalent
2 fast diodes 800 V/1 A, BY 500-800 or equivalent
5 Zener diodes ZPY 100
2 Zener diodes ZPD 6,2
1 Zener diode ZPD 9,1
1 Zener diode ZPD 2,7
1 Zener diode ZPD 5.6
2 fast power diodes BYW31 - 100 V (Motorola) ($I_D = 25$ A, $V_R = 100$ V, $\tau \leq 200$ nsec)
1 Thyristor 50 V/15 A
Universal diodes 1N4148 or equivalent
1 universal diode BAX14 ($I_F \geq 400$ mA) BAX 18
1 opto coupler CQY80 (Telefunken)
1 control IC TL494 (Texas, Motorola)

Capacitors

3 x 2200 pF 250 V VDE (foil or ceramic)
1 x 0,22 µF 250 V VDE (foil)
1 x 0,22 µF/630 V
1 x 47 nF/630 V
2 x 220 µF 385 V electrolytic (standing)
2 x 2200 pF 1500 V impulse-proof (bipolar version) or 680 pF 1000 V ceramic
all other capacitors, foil at 100 V or electrolytics at 25 V

Resistors

1 x NTC resistor K 231/4,7 Ω or better K 232/33 Ω (Siemens)
1 x VDR resistor SØ7 or S2Ø K250 (Siemens)
wirewound 7W/4W (Vitrohm otherwise carbon/metalfilm 0,25 W if required 0,5 W RM10.

Heatsinks

Power Transistor: 2 finger-finned bolted together or alu. diecast finger-finned 5 K/W e. g. Fischer FK318

Dioden: Heatsink 100 x 65 x 25 mm, e. g. Fischer SK 18

Transistor heat sink about 50 K/W for driver 2N2219

3.3. Printed Circuit Board DB1NV 002

The construction can now proceed in accordance with the circuit schematic and component layout **(fig.6).** There are however, a few points to watch:-

The bipolar transistor version, now under consideration, has a slow-rise-network load resistance comprising three parallel 3,9 Ω /7 W resistors. In order to prevent scorching of the PCB and heating of the power transistor, these resistors should be arranged to be physically above the component plane. This is accomplished by soldering two 5 cm long pieces of 1.5 mm wire in the solder points on

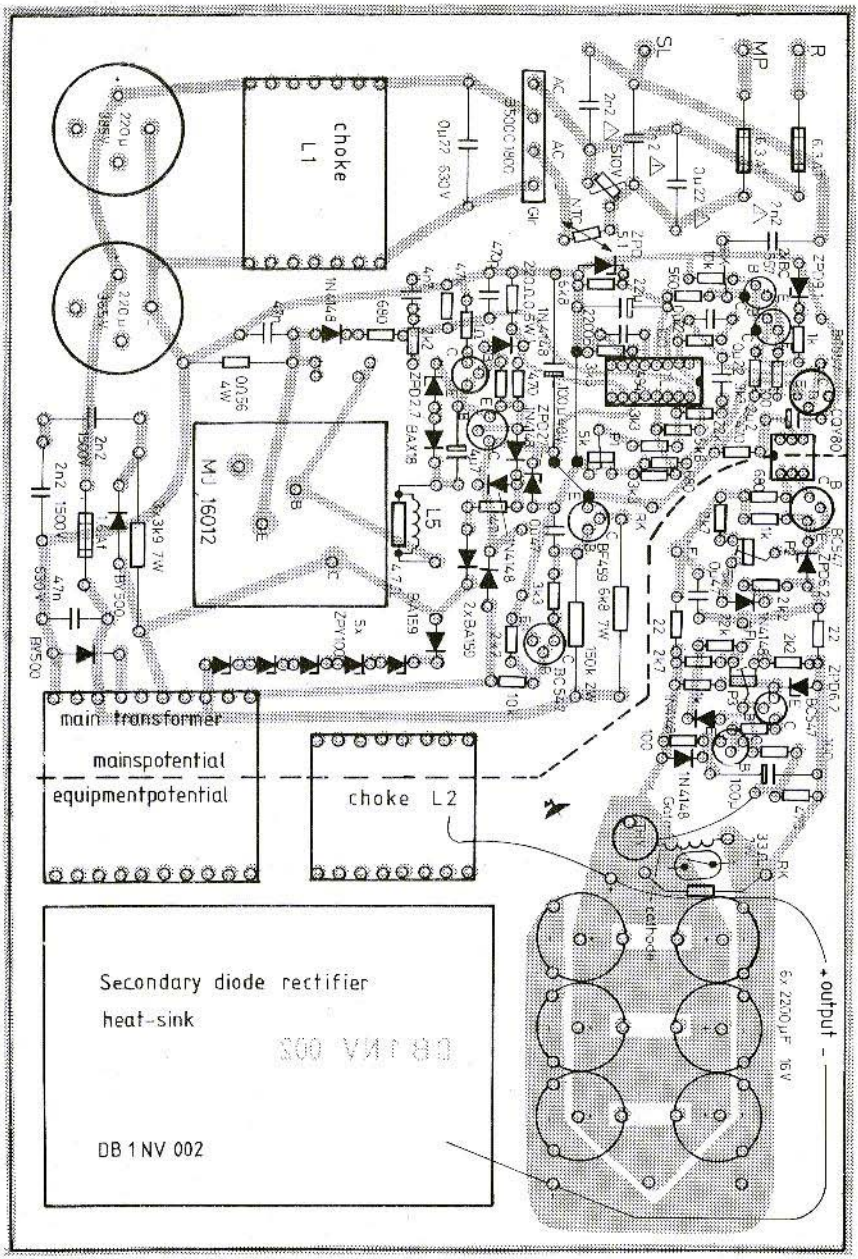

Fig. 6: Component plan and conductor bands of 37 single-sided 280 mm x 190 mm DB1NV 002 PCB for switched-mode supply

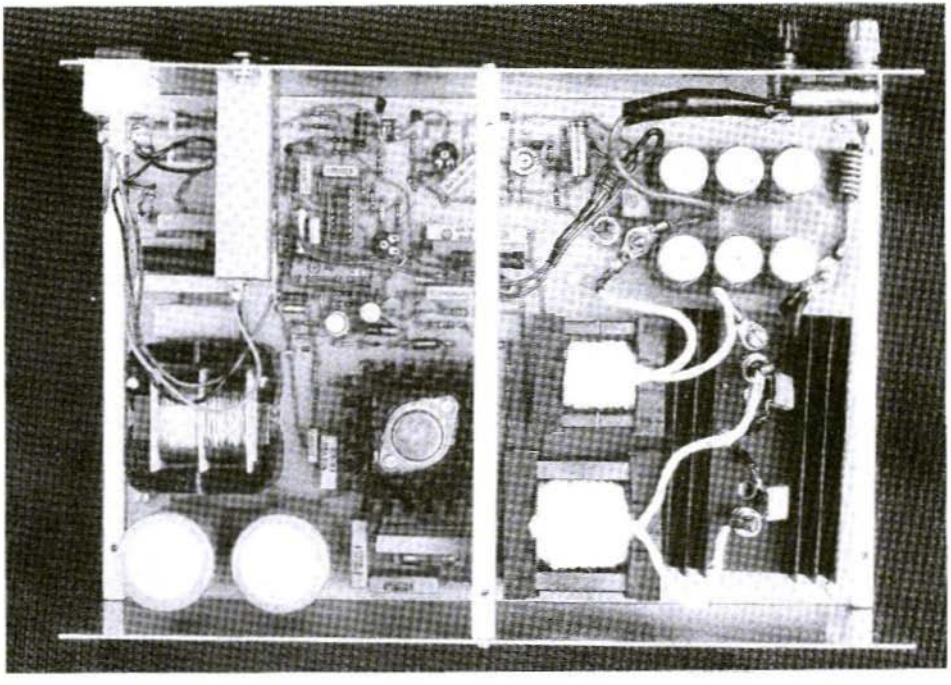

Fig. 7: Test construction of SMPS DB1NV 002

the PCB. The resistors are then soldered between, ladder-fashion, with a 2 cm clearance to the PCB's surface. This may be seen from the photo **fig. 7** of the underside of the prototype.

The "high-current" wiring of the transformer secondary is not taken via PCB tracks but directly to the capacitor connections and secured with M 4 brass screws, the heads of which, are soldered to the PCB tracks. The photo should indicate the general arrangement.

The damping components of the secondary diodes are connected with one end to a solder-tab screwed to the heatsink and the other end directly to the diode anode.

The suppression filter capacitors at the DC output are also connected directly to the component terminals. For chokes L 3 and L 4 there are two suggestions:
either slip two suitable sized tubes over the conductors or use transformer paper and secure with 3 to 5 turns of 2,5 mm CuL.

It is of great importance that the reed relay, used to initiate the slow-start at the moment of ignition of the over-voltage protection thyristor, is correctly provided. Two Litz-connecting wires are carefully soldered to a large ($l \approx 40$ mm) reed contact and insulated with heat-shrink tubing. In the middle of the reed contact 3 to 4 turns of 1 mm CuL wire are wound which form the excitation-coil in the thyristor's cathode. The windings are secured with two-component glue to the contact before the assembly is pressed into service.

The simplest form of housing is provided by a U-formed chassis of 1,5 mm aluminium plate with a cover of thin perforated sheet. It is recommended that the chassis is stiffened by two square cross-section (8 x 8 mm) lengths of aluminium as shewn in **fig. 7.**

4. ADJUSTMENTS

Before the completed supply can be used, it must be very carefully adjusted and tested. For this, an oscilloscope, an adjustable isolation transformer and a current limited test, DC power supply 0 - 20 V/0,5 A are required.

The over-voltage protection on the secondary side is adjusted first by applying 15 to 16 V to the output terminals and adjusting P 3 so that the thyristor fires at 15,5 V and the output voltage is thereby short-circuited.

With P 1 and P 2 set to mid-position, the test-supply is connected between pin 11/12 (+ Ve) and pin 7 of the TL494. The oscilloscope is connected to pin 5 of the TL494. The test-supply voltage is slowly raised from zero to about 12 V. At a potential of 7 to 8 V a saw-tooth waveform should be seen at a frequency of 100 to 120 kHz.

The oscilloscope is then connected to pin 10, which is at this time, at ground potential. Increasing the test-supply voltage to just above 12 V (the over-voltage protection threshold) a square wave train is displayed which has a frequency of 50 to 60 kHz with a duty-cycle varying between zero (shut down) to almost 50 % (full output). When a short-circuit of the reed-relay occurs the impulses disappear and when it is removed the duty-cycle increases to almost 50 % thus providing the necessary slow start.

The same pulse train is to be seen at a lower amplitude at the base of the switching transistor. Check also the reference voltage of 5 V at pin 14 of the TL494.

The high voltage portion will now be tested: – The test-supply is disconnected and the base of T 4 connected to the emitter of T 5. The collector resistor of T 4 is also disconnected. This puts the starting circuits out of action.

The power-supply is now connected via a variable isolation transformer to the mains supply and the voltage slowly raised. The input current should be about 20 mA at 220 VAC representing mostly the reactive current through C 2. The reservoir capacitor then has a voltage of about 300 V across it.

The start circuits are now rendered operational again (but wait for the charge on C 5 and C 6 to decay) and the input supply raised once more to 220 VAC. The output voltage is then adjusted to about 13 V by means of P 2 and the current-limiter to 20 A with P 1.

When doing this, the current limiting foldback characteristic must be taken into account. This facility reduces the over-current in the output circuit to long-term, safe proportions. It can also prevent the power supply from feeding low resistance loads, such as incandescent lamps, under test conditions. In normal use, (transceiver switched to receive) the power supply starts reliably with to 5 A initial load.

5. HOUSING AND OPERATION

The PCB should be installed in a screened metal enclosure as may be seen in the picture of the prototype. The construction does not need to be absolutely "watertight" because of the relatively low frequency of the interference likely to be present. The radiation of internally generated interference is dependent mainly upon the power being supplied.

The mains filter, mains on/off switch and output terminals may be mounted on the side wall of the chassis. It should be mentioned again, at this stage, that the suppression components on the PCB represent only the minimum necessary which, in any case, should be completed with a good mains filter.

The rectifier and transistor heat-sinks are generously dimensioned for "normal" radio communication operation and should work continuously at

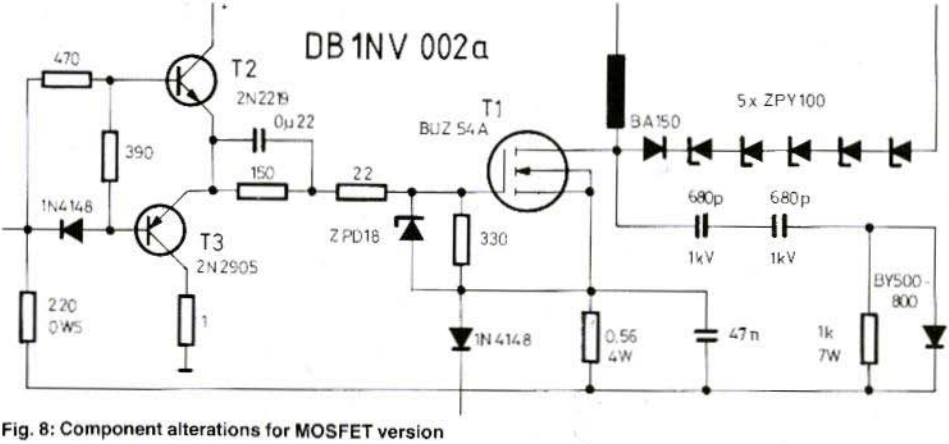

Fig. 8: Component alterations for MOSFET version

10 to 15 A under good ventilation conditions. Should continuous full loads of 20 A be required at higher ambient temperatures, larger heat-sinks or forced-air cooling should be provided.

6. ALTERNATIVE PROVISION OF POWER-FET

The PCB has been provided with the means by which a power-FET may be fitted with the minimum of alteration. The power-FET chosen for the prototype was the Siemens BUZ 54A $V_{DS} \geq 800$ V, $I_{DS} \geq 4$A. As the circuit-extract of **fig. 8** shows, the driver stage is merely wired differently, the anti-saturation components are not required and the drain RCD network components are considerably smaller. Whereas the bipolar transistor losses arise mainly from the finate switching times and are not so dependent upon the load, the FET losses are almost entirely I_D^2 losses which occur during the conducting period of the FET. It is therefore to be expected that the FET with a light load-current, works at the higher efficiency and that the bipolar efficiency is greatest at full load. In between these extremes, both types of transistors behave in the same manner as may be confirmed by the data in the following paragraph.

7. MEASURED VALVES AND USER EXPERIENCE

Prototypes of both FET and bipolar versions of the switched-mode-power-supply were constructed and tested. The following data was obtained.
Mains input 220 VAC. Output voltage 13 VDC
Quiescent current (bipolar) = 15,5 W
Quiescent current (FET) = 8 W

Table 1 shows the comparative efficiencies of both supplies at various load currents.

I_L/Amps	2	5	10	15	20
ε/% bipolar	63	86	86	87	86
ε/%	78	89	93	91	87

Table 1

As it can be seen, the FET version is slightly more efficient under partly loaded conditions. The switch-on surge current of the supply was limited to about 10 A by a thermistor. Without the thermistor and with only the input choke, the surge current rose to 30 A. The periodic peak current from the mains supply was about 4 A at full load. With the heatsinks as shown in the photograph, the important components such as switching-transistor, secondary diodes, transformer and choke reached a temperature of 50° C under 10 A load conditions. Only the slow-rise network resistor was warmer with a temperature of 80° C. After these tests were conducted, both supplies were put into service by DL 8 MX. The "test load" was an ICOM IC 730 with a L7B power amplifier into a Periodic-7 beam. Despite the close proximity of the power supply to the radio equipment – it was laid directly on the PA in order that the 12 V cables would be of minimum length – no signs of HF interference was apparent on any band. Using the TS 930 receiver portion there was also no evidence of power-supply switching frequency harmonics. Experiments with VHF/UHF transceivers and PAs were also as successful. The only source of annoyance was the distorted sidetone, which was to be heard from the ferrite cores, which had not been glued on the prototype.

Summary

With normal over-the-counter components, a 12 V switched-mode-power-supply (SMPS) with an overall size of 300 x 200 x 70 mm^3 and just 3 kg in weight can be realised. It may be used to supply all the customary transceivers with the necessary freedom from either unwanted radiations or from mal-function arising from RF fields.

Drs. Tjapke Knoeff, PAØ

FM/AM Converter for Facsimile Reception and Picture Display with the YU3UMV Picture-Store

This small circuit converts the frequency-modulated transmitted facsimile (FAX) signal into an amplitude-modulated 2400 Hz tone. This enables the well-known weather satellite, picture-store (WEFAX) module YU3UMV 001/002, to be used for these transmissions.

1. CONCEPT

The WEFAX picture-store described in (1) is actuated by an amplitude-modulated 2400 Hz tone from the radio receiver. In order that the picture-store may be used, without modification, for FM FAX transmissions, the following module is employed to convert the receiver FM output into a suitable AM output. Naturally, there are circuits concepts which would route the signal around the AM stage directly to the analog/digital converter, but that would entail alteration to the circuitry of YU3UMV 001, and the object is, to avoid that. The concept to be followed also has the advantage that with separate converters, the recovered AM signal can be stored on an ordinary cassette-recorder. This is not possible with the demodulated FM signal because the 2400 Hz tone is used for picture store synchronizattion.

2. CIRCUIT DETAILS

Figure 1 shows the simple circuit of this small module. The incomming FM signal deviates ± 400 Hz from a carrier whose mid-frequency is 1900 Hz, i. e. 1500 Hz represents the black and 2300 Hz represents the white on the picture to be displayed.

The Plessey SL 1626 is an integrated compressor with a large degree of regulation which effectively suppresses all traces of amplitude-modulation, which may be present on the received FM signal. The four-stage, 10 kΩ / 4,7nF AF low-pass filter exhibits a 12 dB per octave attenuation above about 2400 Hz. Its purpose is to limit the effect of impulse and sideband noise from the circuits which follow. The output from the third, LM 324 amplifier, IC 3 is fed to the PLL demodulation LM 565. The VCO frequency is determined by R 1 and C 1 at 1900 Hz according to the formula: –

$$f_{VCO} = 1/(2{,}7\ R_1\ C_1)$$

This frequency may be checked at (high impepance) pins 4 and 5 of the LM565.

The demodulated signal encounters a further low-pass filter (R 2, C 2, C 3), before being amplified

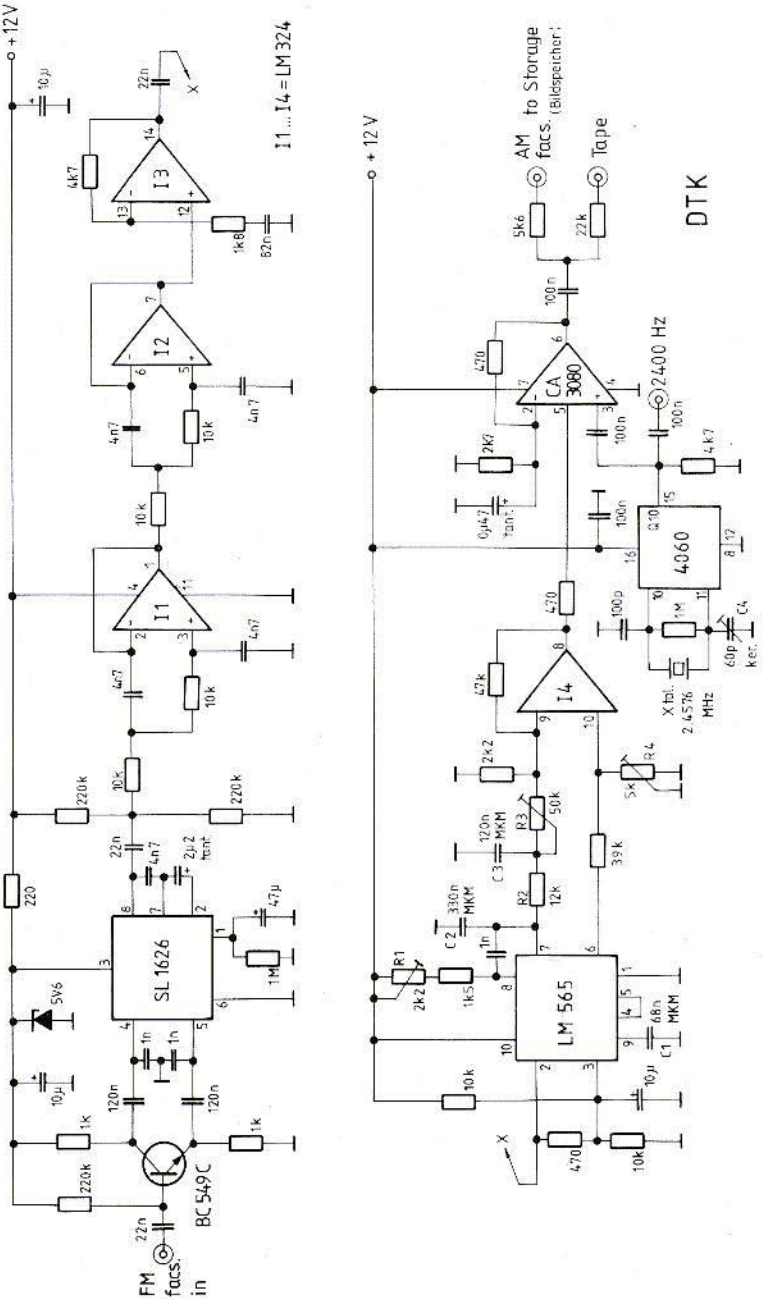

Fig. 1: FM/AM converter for FAX reception

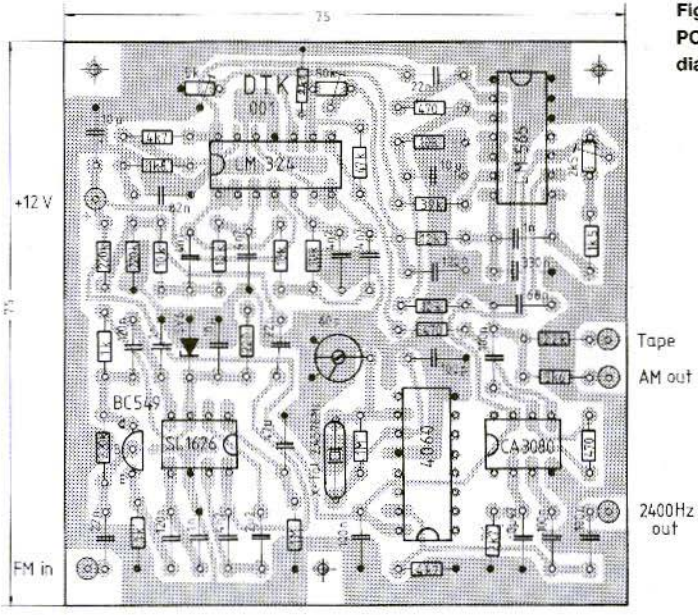

Fig. 2:
PCB for circuit diagram of fig. 1

by a fourth op. amp. IC 4. A CA 3080 functions as a modulator at 2400 Hz, this frequency being derived from a 2,4576 MHz crystal by a 1024 divider. The 2400 Hz tone is taken to an auxiliary output for synchronization of METEOR weather satellites. The trimmer C 4 is adjusted in order that the METEOR picture is exactly vertical on the monitor screen. A tape output is provided via a 22 k Ω isolating resistor, enabling the AM signal to be recorded.

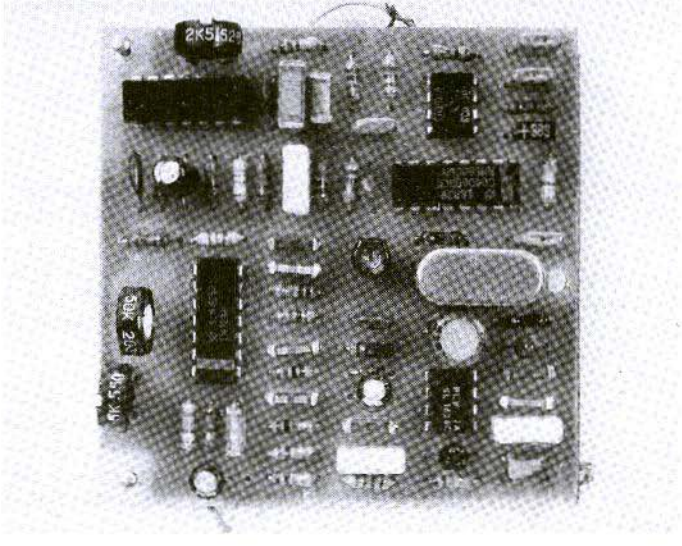

Fig. 3:
A completed example of the converter

3. CONSTRUCTION

A single-sided PCB 75 x 75 mm has been designed for this circuit and is shown in **fig. 2**. A completed example is shown in the photograph of **fig. 3**. A few words about the components: The crystal is provided with a holder HC-6/U and the oscillator and filter capacitors are foil-types with a pin-spacing of 7,5 mm. The three trim-pots are upright types with a pin-spacing of 5/2,5 mm and the trimmer capacitor C 4 can have a diameter up to 10 mm.

4. CONCLUDING COMMENTS

To check and to demonstrate the function of this converter with the YU3UMV picture-store, the professional station Bracknell (3,2895 MHz), DPA (139,6 kHz) or DCF 54 are suitable. They send photographs and weather satellite pictures, but sometimes with a frequency deviation of only 150 Hz. The trimmers R 3 and R 4 then have to be readjusted.

Should the picture appear negative on the monitor screen the other sideband of the received signal should be selected. It is surprising how even scarcely audible, QRM-plagued signals are still capable of delivering a recognisable picture.

5. REFERENCES

(1) Vidmar, M.:
A Digital Storage and Scan Converter for Weather Satellite Images
Part 1: Electronic Module
VHF COMMUNICATIONS Vol. 14, Ed.4/82
Pages 194-208

A Digital Storage and Scan Converter for Weather Satellite Images
Part 2: Storage Module
VHF COMMUNICATIONS Vol.15, Ed.1/83
Pages 12-25

Ben Simon, EMS Israel

The METEOSAT-monitor can easily be made to display a sector which is only 1000 km square.

The YU3UMV digital picture store, universally used by radio amateurs, is easily modified in order that a X4 magnified sector appears on the screen. It functions without any geometrical distortion with METEOSAT and METEOR transmissions at 240 lines per minute.

- The x0,5 function is sacrificed and this switch contact is instead connected to the sync.-frequencyof 38,4 kHz.
- A further switch contact is required in order to connect I 219 pin 6 (YU3UMV 002) to ground. This prevents the lines being written on top of one another.
- Some equipment had to be modified in order to increase the sync.-frequency of the AD-converter ADC 0804 to enable a clean conversion at the new rate of 208 ns per pixel.

One requires, of course, some operating experience in this mode in order to slide the horizontal start point onto the required strip of interest. An adjustable (switchable) monoflop which delays the line pulse to the desired point can help in this respect.

Matjaž Vidmar, YU 3 UMV

Polarization Performance of Circularly Polarized Antennas

In the early days of radio-amateur experiments, all long distance contacts were made in the high frequency range using skywaves. Since the ionosphere also has a very strong influence on the polarization of radio waves (Faraday rotation and other effects) and the ionosphere itself is continuously changing, there is no easily observable relationship between the polarization of the transmitted wave and the polarization of the received wave. As a consequence, little if any, care was taken about the polarization of the antennas used. In the VHF and higher frequency ranges, most contacts are made in line of sight, or almost line of sight conditions and the relationship between the polarizations of the transmitted and received waves can easily be observed.

Most amateurs only use horzontal linear polarization for long distance SSB/CW contacts and vertical linear polarization for local / repeater FM contacts. In the satellite communications field and in some other more specialized areas, circular polarization, either righthand or lefthand or both are used. Of course, there is no "ideal" polarization but one can always find a polarization that is the most suitable for a particular application.

1. CIRCULAR POLARIZATION AND ITS PROBLEMS

The theory states that, given an arbitrary polarization one can always find a polarization orthogonal to this polarization. The word orthogonal does not necessarily have a geometrical meaning (as in the case of horizontal and vertical linear polarizations), it simply says that two orthogonally polarized waves are completely independent: using suitable equipment two independent information channels can be carried in the same frequency band without mutual interference. On the other hand, this means that it is not possible to build an universal antenna with a single output capable of receiving any incoming wave without any switching, or any other changes in the antenna itself. The theory also states any arbitrary polarized wave can always be generated as a complex weighted sum of two orthogonally polarized waves.

With a couple of orthogonally polarized antennas

one can therefore receive and transmit with any polarization!

In a typical radio link there are many causes that affect the polarization of the signal and as a consequence its performance. These can be divided into two groups: propagation path effects and inaccuracies of the two antennas. While little can be done to counter the propagation path effects, the construction, alignment and testing of suitable antennas deserves attention. The polarization performance of an antenna can be described in various ways: for example, as the ratio between the desired wave and the unwanted orthogonally polarized wave, which is also called cross polarization rejection ratio (CPRR) and is usually given in dB.

In the VHF and lower UHF frequency range popular **linearly** polarized antennas such as dipoles, yagis, log periodics, and various arrays of these antennas, usually have a very good CPRR. The thin wire (rod) structure of these antennas forces the RF currents to flow along the wires (rods), therefore it is quite easy to control the direction of the generated E field. Since a good CPRR is already guaranteed by the physical construction of the antenna itself, it is usually not even specified in the data sheet of the antenna.

On the other hand, it is considerably more difficult to make a good **circularly** polarized antenna. A long helix (10 turns) may have the CPRR as poor as 15dB. If circular polarization is to be obtained from two orthogonally linearly polarized antennas (yagis), just a slight mismatch in the feeding network may cause an even worse CPRR.
In a perfect circularly polarized wave, the E field vector describes a perfect circle. However, if a small amount of the orthogonally polarized circular component is present, the E vector no longer describes a circle, it describes an ellipse. The axial ratio (AR) of this ellipse represents another way to describe the polarization performance of a circularly polarized antenna. The axial ratio (AR) also is usually given in dB. Its main advantage over the CPRR is that it can be easily measured using a linearly polarized probe.

The relationship between the AR and CPRR becomes very simple if both of them are expressed in linear units (voltage or E-field ratios, not dB!):

$$AR = \frac{CPRR + 1}{CPRR - 1}$$

In the VHF range the dimensions of a helix antenna, in particular its reflector, become unpractically large. A practical solution to obtain circular polarization is to use a pair of properly fed, crossed dipoles or yagis. Usually it is only necessary to provide an additional 90° phase shift for one of the two antennas, either using a $\lambda/4$ longer (or shorter) feedline (**fig. 1.**) or physically shifting one antenna.

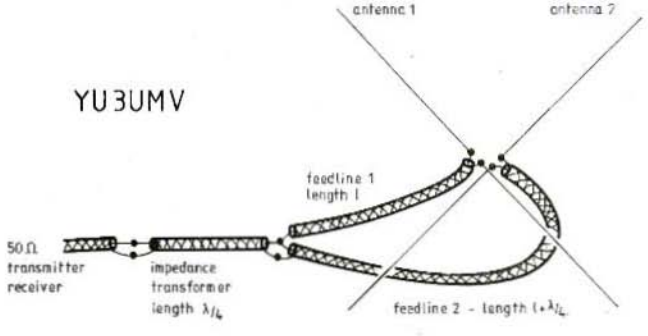

Fig. 1:
Feeding two linearly polarized antennas with different length feedlines to obtain circular polarization.(Baluns and other matching hardware of the single antennas are omitted for simplicity!)

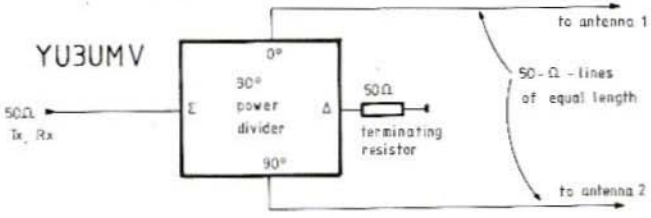

Fig. 2:
Feeding two linearly polarized antennas with a 90° power divider (coupler) to obtain circular polarization.

Of course, to obtain a good circular polarization the two antennas must be practically identical. This is especially important in the case of tolerance sensitive yagi antennas: note that the two antennas must be matched both in amplitude and in phase! Unfortunately a careful mechanical construction of the antennas and a correct installation (using rods or tubes made of insulating material for all the support structures which are not perpendicular to the generated E field) are necessary but not sufficient to obtain a good circular polarization.

To obtain a 90° phase shift, most amateurs simply connect the two feedlines (one being $\lambda/4$ longer than the other) in parallel and then match the impedance obtained to the impedance of the transmitter or receiver with a suitable $\lambda/4$ transformer (**fig. 1**). A perfect circular polarization is obtained only if both antennas are perfectly matched to their feedlines. Just a slight mismatch of one or both antennas will cause a very poor axial ratio. Since the two antennas must be of identical construction, one can also expect a similar reflection coefficient or SWR. At the other end of the two feedlines, the reflection coefficients are still similar in amplitude, but due to the different lengths of the feedlines their phases differ by almost 180°. This causes an unequal power division, both in amplitude and in phase. Since the two antennas are not fed with equal amplitude signals and the phase between the signals is not 90°, the resulting wave will certainly not be perfectly circularly polarized.

Assuming that the two antennas are completely identical and thus have the same SWR and that the losses in the feedlines are zero, the expression to evaluate the axial ratio (AR) becomes very simple: the AR is directly proportional to the SWR:

$$AR = VSWR$$
$$AR[dB] = 2Ø \log VSWR$$

But what is the practical meaning of this result? A VSWR value of 2 is usually still accepted at the band limits of a certain antenna. Two such antennas will however give a very poor axial ratio of 6 dB! This highly elliptical polarization, is actually almost closer to linear polarization than to circular polarization.

If the antenna system has to operate in a wider frequency range and variations of the SWR across the frequency band can hardly be avoided, then a 90° power divider has to be used as the feeding network with the fourth (difference) port terminated with a resistor (**fig. 2**). The main disadvantage of this solution is that part of the transmitter power is dissipated in the terminating resistor. Most amateur antennas only work over very narrow frequency bands, therefore even the simple feeding network with different cable lengths (**fig. 1**) can be adjusted to give a good circular polarization. Of course, one should be able to measure SWR with a reasonable accuracy. Note that many low cost reflectometers available on the amateur market, marked 3 to 150 MHz on the front panel, show a SWR of 1,5 or even 2 when terminated with a precision microwave 50 Ω resistor at 144 MHz! Therefore, before starting any adjustments check the accuracy of your SWR meter!

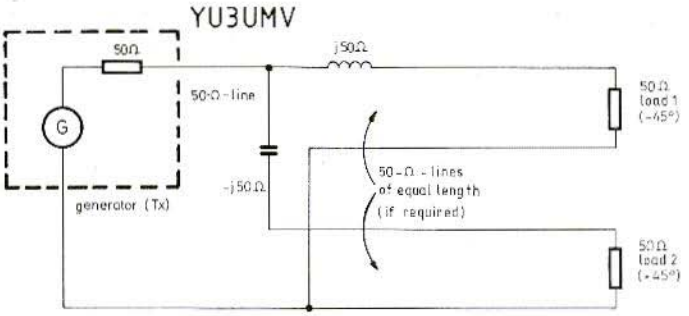

Fig. 3:
Feeding two linearly polarized antennas with a matching network made of lumped components to obtain circular polarization.

2. A PRACTICAL PROPOSAL

On a practical note, I would like to demonstrate a very simple method to obtain a 90° phase shift and a perfect impedance match of two orthogonally polarized 50 Ω antennas to a 50 Ω source. If the antenna system is only used for reception and/or for low power transmission up to 50-100 W, the required phase shift and impedance match can easily be achieved by two lumped components (**fig. 3**). A reactance of -j 50 Ω corresponds at 145 MHz to a capacitor of 22pF. A j 50 Ω inductor can easily be found with a GDM, since it must resonate at the operating frequency with the capacitor. A perfect impedance match to a 50 Ω transmitter is guaranteed since:

$$Z_1 // Z_2 = \frac{Z_1 Z_2}{Z_1 + Z_2} = \frac{(50 + j50)(50 - j50)}{(50 + j50) + (50 - j50)}$$

$$= \frac{2500 - j \cdot j \cdot 2500}{100} = \frac{5000}{100} = 50\ \Omega$$

If switching between RHCP and LHCP is required the circuit has to be modified according to **fig.4**. Note that a single switching contact is required and that the stray capacitance between the open contacts should be subtracted from the calculated value.
The whole circuit becomes even more simple if the two antennas are fed with a "gamma-match". A gamma-match already requires a series capacitor to tune the antenna to 50 Ω. It is only neces-

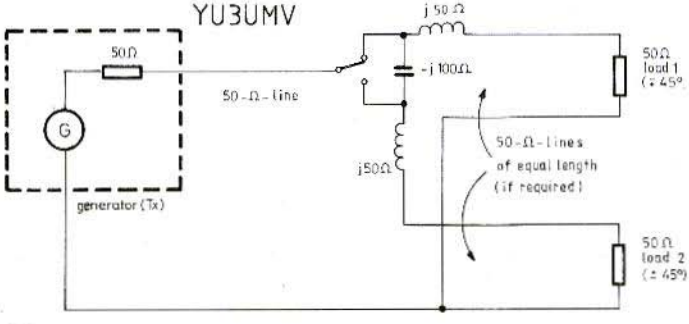

Fig. 4:
Modified circuit to enable switching between RHCP and LHCP.

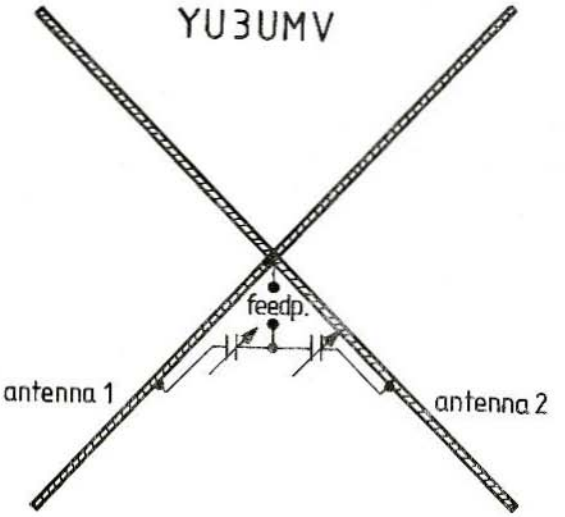

Fig. 5:
Feeding two antennas with a gamma-match".

sary to modify the values of these capacitors and then simply connect the two antennas in parallel to get a 90° phase shift and 50 Ω generator matching at the same time (**fig. 5**).

The procedure to align the two variable capacitors is as follows:

1.) Connect only one antenna to the transmitter and by adjusting both the variable capacitor and the dimensions of the "gamma-match", an SWR of 1 should be obtained.
2.) Connect only the other antenna and repeat the same procedure as in step 1.) to obtain an SWR of 1. If about the same dimensions and capacitance of the "gamma-match" are obtained, it is a verification that the two antennas are sufficiently similar.
3.) Now both antennas are matched to 50 Ω each, any further adjustments will only affect the capacitors.
4.) Connect the antenna that should receive a -45° phase shift (lag) and detune the capacitor, **increasing** its value to obtain a SWR 2.62 which now corresponds to an impedance of (50 + j50) Ω. If a SWR of 2.62 cannot be obtained even with very high capacity values, the capacitor has to be replaced with an inductor. An alternative but more elegant solution, is to build the "gamma-match" using a thinner wire and repeat steps 1.), 2.), 3.) and 4.).
5.) Connect the other antenna that should receive a +45° phase shift (lead) and detune the capacitor, **decreasing** its value to obtain a SWR 2.62 which now corresponds to an impedance of (50-j50) Ω.
6.) Connect both antennas in parallel and verify that the SWR is close to 1.
7.) Check wether you have obtained the desired polarization, either RHCP or LHCP, since it is very easy to make mistakes with the phases of the individual antennas.

Erich Stadler, DG 7 GK

The Directional Coupler Function and Use

By means of the directional coupler, the reflection from amplifier inputs, impedances, and in particular, from transmitter antennas can be determined. If the coupling coefficient is known, this measurement device is suitable for the measurement of transmitted power and the reflected power from the antenna.

1. TEST SET-UP

The arrangement in **Fig. 1** consists of two directional couplers connected in series, and a signal

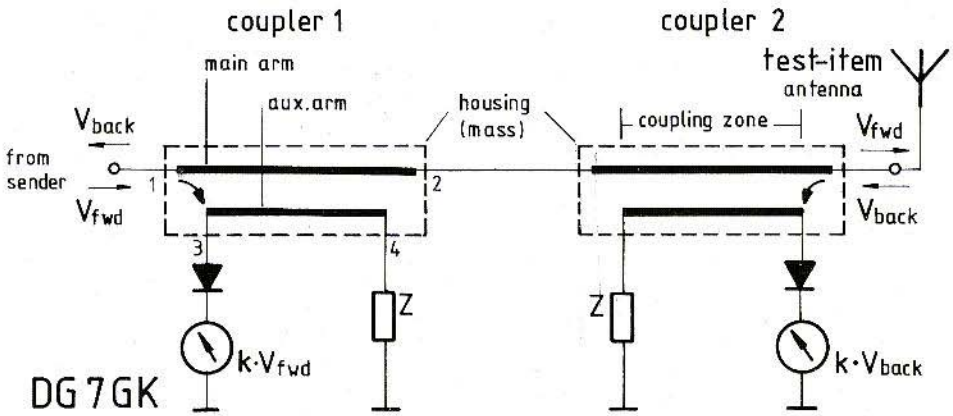

Fig. 1: Reflection coefficient measurement set-up

generator. The signal is fed to the input of one of the couplers. The item-under-test (IUT) is connected to the output of the second coupler. Each coupler has a third connection, the so-called coupled output, which is used for the measurement. The fourth connection is terminated in Z.

1.1. Coupler Construction and Function

A directional coupler has a so-called main arm and an auxiliary arm. Both are mutually coupled such that a fraction of the power in the main arm is coupled into the auxiliary arm. The peculiarity of the directional coupler is that the coupled power is not available at either one and/or other of the auxiliary arm connections but **only at one**, the other output being "completely" decoupled. The question of which is the coupled and which is the decoupled output depends entirely upon the direction of power flow in the main arm! The reason for the existence of a decoupled output lies in the mixed coupling, namely capacitive and inductive coupling between main arm and auxiliary arm.

1.2. Basic Diagram

The main arm **(Fig. 2)** lies between connections 1 and 2 and the auxiliary arm between 3 and 4. The larger the separation between main and auxiliary arm, the smaller the coupling coefficient is, i.e. the greater the coupling loss (20 log I/k, dB). The

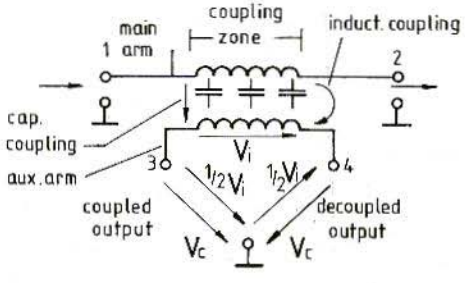

Fig. 2: The coupler's basic diagram

source voltage V_{fwd} at (1) produces a power flow to output (2) which is terminated in either the antenna or a second coupler. V_{fwd} produces by means of capacitive coupling a voltage which is uniformly distributed along the auxiliary arm with respect to (w.r.t.) to ground, and in particular at points 3 and 4 has the same direction w.r.t. ground. The signal due to inductive coupling is, however, different. The main and auxiliary arms may be considered as being the primary and secondary of a transformer in which the voltage across the primary is induced into the secondary V_i. The terminations at outputs 3 and 4 form together with the auxiliary arm itself a bridge circuit across which the secondary voltage V_i divides equally between outputs 3 and 4 with the directions shown in **Fig. 2.** It may be seen that at 4 the voltages V_c and V_i are anti-phase, and at port 3 are in phase. By suitable physical dimensioning, V_i and V_c can be made equal and therefore add at port 3, the output port, and cancel each other at the decoupled, terminated port 4.

Example

A transmitter delivers 10 W in 50 Ω. Its output is connected to a directional coupler with a coupling loss of 20 dB. What is the voltage in the main arm? What is the voltage in the coupled output?

Solution

Voltage in main arm $V_1 = \sqrt{10W \times 50\Omega} = 22.4$ V
Coupling coefficient: 20 dB means a voltage ratio 10 : 1. The coupling coefficient is then 1/10 = 0.1. At the coupled output the voltage $V_3 = 22.4$ V x 0.1 = 2.24 V (across a coupled output port impedance of 50 Ω).

1.3. Frequency Dependence of Coupling Coefficient

The coupling coefficient k, and with it the coupling loss, is not constant but dependent upon frequency, as **Fig. 3** shows. The maximum coupling

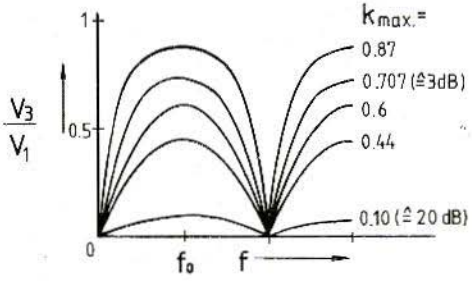

Fig. 3: Frequency dependence of coupling coefficient $k = V_3/V_1$

coefficient k_{max} is obtained when the "coupling zone" is suitably dimensioned. The coupling zone is the length of the coupler conductors over which coupling takes place. Maximum coupling k_{max} occurs when the coupling zone is a quarter wavelength. At low frequencies this means very large coupler lengths particularly when the coupled conductors are spaced in air and no reduction due to velocity factor is possible.

Example

Length of a λ/4 coupler at 145 MHz:
a) Insulation air,
b) Polyethylene ?

Solution

λ = 2 m
a) Coupler length 2 m x 1/4 = 50 cm
b) Velocity factor for PE is 0.66 therefore coupling length is only 50 cm x 0.66 = 33 cm.

Fig. 3 shows that a coupler is not broadband inasmuch that it may be dimensioned for one frequency and used at another frequency with the same facility. It has at other frequencies, among other considerations, a different coupling loss.

Example

A quarter-wave coupler has been designed for a mid-band frequency of 435 MHz at a coupling loss of 20 dB.
a) To which k_{max} does this correspond?
b) The coupler is also used at 145 MHz. What is the coupling loss at this frequency?

Solution

a) $k_{max} = 1/10^{20/20} = 0.1$
b) At small coupling coefficients k_{max} the curves in **Fig. 3** approximate a sinewave
$k = k_{max} \times \sin(90° \, f/f_0)$,

where f_0 is the mid-band frequency of the quarter-wave coupler. This results in an actual coupling coefficient at 145 MHz of:
$k = 0.1 \times \sin(90° \times 145 \text{ MHz}/435 \text{ MHz}) = 0.05$.

This corresponds to a coupling loss of 26 dB, i.e. 6 dB more than at f_0!

NOTE: The exact formula for the coupling coefficient V_3/V_1 is:

$$k = \frac{k_{max} \times \sin(90° \times f/f_0)}{\sqrt{1 - k_{max}^2 \times \cos^2(90° \times f/f_0)}}$$

and results in the curves given in **Fig. 3**. In order to calculate the mid-band frequency f_0 from the given coupling zone length l_k and the velocity factor V_k, the following formula is used:

$$f_0 = \frac{c \times V_k}{4 \times l_k}$$

where c is the velocity of light 300×10^6 m/s

2. APPLICATION

2.1. Measurement of the Reflection Coefficient (Fig. 1)

Two identical couplers are used with **the same**

coupling coefficient k. A voltage k x V_{fwd} proportional to the forward wave, is measured at an output of coupler 1. At the output of coupler 2, a voltage k x V_{back} proportional to the reflected voltage V_{back} is measured. From the ratio k x V_{back}/k x V_{fwd} the coefficient k is cancelled out leaving the "Reflection Coefficient" r.

$$r = V_{back}/V_{fwd}$$

In many test set-ups the outputs from the coupled ports are taken via diode rectifiers to potentiometers the wipers of which are connected to meters. The wipers are ganged mechanically such that if the forward meter for k x V_{fwd} is adjusted to full scale deflection (FSD) the meter k x V_{back} will indicate, as a proportional deflection, the reflection coefficient directly (assuming that both diodes are linear).

With well matched loads the reflected wave amplitude is much smaller than the forward wave. In order to obtain a sufficient sample voltage to measure the **return wave**, a directional coupler with a **lower** coupling loss is frequently employed at transmitter sites.

NOTE: In principle it is possible to use only one coupler, whereby port 4 serves to measure the return wave and port 3 the forward wave. The great danger with this practice is that the output ports are not optimally matched due to the rectifier circuit. This leads to large errors in the measurement of the return wave (see also "Directivity").

2.2. Transmitted Power Measurement

Even when the antenna feeder is lossless, the power radiated is not necessarily that of the transmitter output power. The difference between both powers is all the more when the antenna system is badly matched to the transmitter, i.e. the greater the reflection coefficient is. Prerequisite for a measurement according to **Fig. 1** is a coincidence of the characteristic impedance of the directional coupler, the terminating resistances of the coupler outputs, and the internal impedance of the transmitter. The r.m.s. voltage output of the coupled port is divided by the coupling coefficient k in order to obtain the forward voltage V_{fwd} across the main arm. The absolute value of k must be known which was not the case for the reflection coefficient measurement. The **forward power** is then $P_{fwd} = (V_{fwd})^2/Z$. This is the maximum available power from the transmitter. According to the match at the antenna, a voltage is received at the coupling output of the second coupler which is proportional to the return wave. If this is also divided by the coupling coefficient k, the amplitude of the return wave V_{back} in the main arm is obtained. The **return power** is calculated from $(V_{back})^2/Z$.

The term $(P_{back})^2/Z$ is practically a **reactive power** that is reflected as a result of a poor mismatch at the antenna. Since $(V_{fwd})^2/Z$ is the maximal available power from the generator, one can transpose the formula thus:

$P = P_{max} (1 - r^2)$.

Example:

The coupler for the measurement of the forward wave has a coupling loss of 30 dB ($k_1 = 0.032$) and that for the measurement of the return wave has a coupling loss of 20 dB ($k_2 = 0.1$). At the coupled port output an RMS voltage of 960 mV is measured and at the output of the second coupler a reflected sample voltage of 1 V RMS is measured. The measurement system works with an impedance of Z = 50 Ω. Feeder losses are not taken into account. How much power is radiated?

Solution:

First coupler: Forward wave in main arm V_{fwd} = 960 mV/0.032 = 30 V.

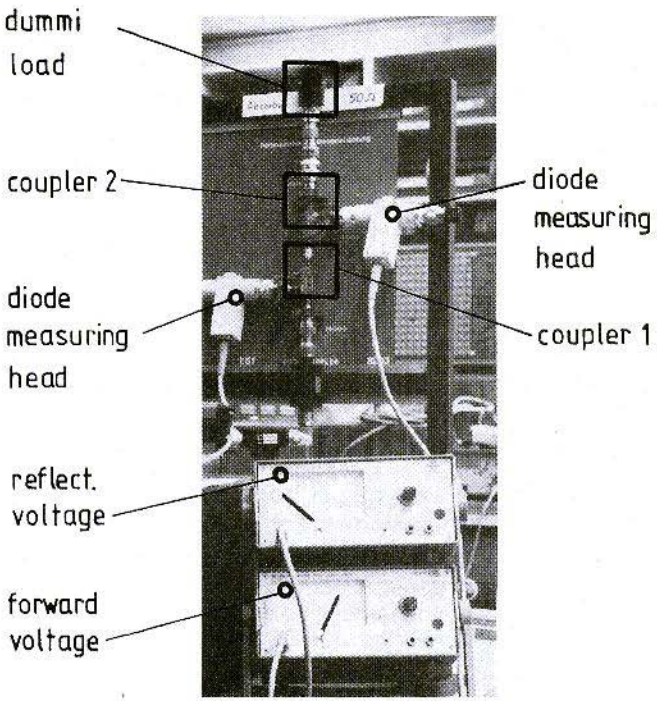

Fig. 4:
Reflection coefficient and power measurement set-up with directional couplers

Second coupler: Return wave in main arm V_{back} = 1 V/0.1 = 10 V.
Forward power: $(30\ V)^2/50\ \Omega = 18$ W
Reflected power: $(10\ V)^2/50\ \Omega = 2$ W
Radiated power from antenna is
P = 18 W – 2 W = 16 W

NOTE: Due to the different coupling losses, a higher voltage appears at the second coupled port in the example than from the first coupler's coupled port. This does not indicate that the return wave is greater than the forward as it might be easily recognized from comparison of the voltages in the main arm. 10 V to 30 V means reflection coefficient of the antenna of 0.33 (33 %).

Despite this, the reflected **power** is not so significant since it is proportional to the **square** of the reflection coefficient. **Fig. 4** presents a reflection coefficient and power measurements test set-up as used at the Electronic School in Tettnang. The nominal frequency range of the 20 dB coupler is 2 to 4 GHz. In **Fig. 4** they are used for a power measurement at 435 MHz.

3. DIRECTIVITY

Due to physical tolerances and non-ideal matching at the coupled ports, it is impossible that

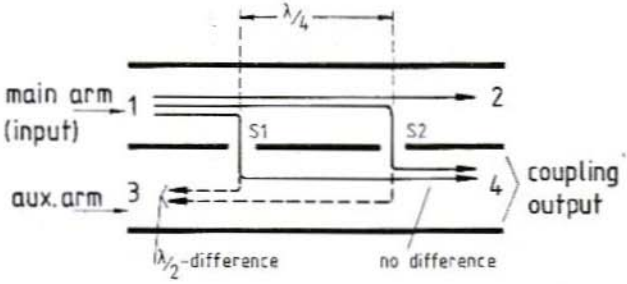

Fig. 5:
Forward wave coupler with waveguides

the decoupled port supplies absolutely no output. In fact, there appears a voltage but a very much smaller voltage than at the coupled port. The ratio of the two auxiliary arm voltages expressed in dB gives the "directivity" which is at least 40 dB for good couplers.

When measuring the forward wave, the consideration of directivity is of practically no interest as the decoupled port is not used since the reflected wave is measured in a separate second coupler. The situation is different with the second coupler which is used to measure a very much smaller reflected wave. As the wave flow in the main arm is in the opposite direction, the measurement port for the reflected wave is simultaneously the "decoupled" port for the forward wave. Should the decoupling be insufficient relative to the forward wave, i.e. the directivity is too small, an interfering signal is present at this port which is superimposed on the wanted return wave leading to very large errors in the measurement. A numerical example will make this clear.

Example

In a test set-up, a coupler with a 20 dB coupling loss (k = 0.1) and a 29.5 dB directivity was employed. The main arm forward wave may be 30 V and the reflected wave 10 V which indicates a reflection coefficient of 0.3. What is the effect of the forward wave upon the reflected wave at the measurement port (measurement error ?)?

Solution

The measurement port signal due to the return wave is 10 V x 0.1 = 1 V. For the forward wave, the other auxiliary arm output of this coupler is the coupling output, which is fed with a voltage of 30 x 0.1 = 3 V. This voltage does not interfere since the port is not used. Due to the given directivity of 29.5 dB, 1/30th of the calculated 3 V, i.e. 0.1 V, is present at the measurement port together with the wanted signal of 1 V. The phase of these two voltages determines how much the wanted signal is influenced. In the extreme case, with either in-phase or anti-phase conditions, the measurement error amounts to ± 0.1 V/1 V x 100 % = ± 10 % in this example. Should the reflection coefficient require to be determined within a measurement error of ± 1 %, a coupler with a directivity of 49.5 dB would have to be used instead of 29.5 dB!

The directivity then is an important specification of a directional coupler and has a great impact upon the measurement of the reflected wave.

4. FORWARD AND BACKWARD WAVE COUPLERS

Couplers whose output port lie on the same side as the signal input port in the main arm, are known as backward wave couplers. The foregoing text and diagrams refer to the backward wave coupler.

Another form of coupling is the "Forward wave coupler". This is to be found mainly in waveguide techniques. Its function is easier to understand than that of the backward wave coupler. **Fig. 5** shows the principle. The coupling between neighbouring waveguides is accomplished by small slots spaced by a quarter wavelength. From each slot (S 1, S 2) in the auxiliary arm radiate electrical waves in both directions. In the "backward direction", however, these waves cancel each other because those coming from the second slot have a phase difference to those coming from the first slot of twice a quarter wavelength. The forward wave coupler has therefore port 3 as the decoupled port whilst the wave components at port 4 are in phase and are additive. Port 4 is then the coupled output. Since this lies in the direction of the forward wave in the main arm, the coupler is known as the "forward wave coupler".

5. LITERATUR

Stadler: Hochfrequenztechnik, Vogel-Verlag
Stadler/Ochojski: Messrichtungskoppler, Frequenz 24 (1970) 11

Bernd von Bojan, DJ 7 YE

Determination of Antenna Gain – What's actually behind it all ?

Time and again lately, there have been publications about amateur antenna measurements which give the impression that a high degree of precision has been achieved. In particular, the gain of short-wave antennas and their VHF and UHF models which have been carried out to a few tenths and in some instances to a few hundredth of a dB, have been undertaken. At the same time the gain was determined to within two decimal places in order to accord with the so called "Kraus Formula", which in itself is a rule-of-thumb equation. This situation leads one to the conclusion that the use of the Kraus formula is shrouded in some uncertainty.

It is this problem of the gain of an antenna and its measurement, which this article will address. At the same time, the question of whether highly exact antenna measurements are possible, and even meaningful, will be examined.

Taking short-waves, it is well known, that according to the propagation conditions and the radiation characteristics of the antenna, the received signal varies quite often by more than 30 dB. If highly accurate antenna measurements were technically possible, on account of this, the question must be asked whether such exact measurements are required at all. Nevertheless, if two short-wave antennas are required to be compared with one-another, it cannot be accomplished by an assessment of the free-space characteristics alone. This is because it is not possible to be certain of which components of the antenna characteristic suit a particular distance and elevation above the earth surface.

Short-wave antennas radiate the energy supplied, minus losses, in the space surrounding the antenna. It therefore follows, that by means of ionospheric propagation, the total radiated energy reaches the ionosphere in the ideal case and is reflected from there to a distant point on the earth's surface.

The ionosphere and the earth's surface are decisive factors in the question of how effective the antenna behaves as a radiator.

A short-wave antenna is then a good radiator, if it has the height above ground which is suitable for the ionosphere at an optimum time for the particular path length under consideration. It is a notable fact, that theoretically, two antennas with differing free-space gains will produce the same field strength at a distant receiver. The antenna with the highest free-space gain is not necessarily the most successful.

This is also partly true for VHF and UHF according to what purpose the antenna is being used. (Me-

teor-Scatter: high dispersion, EME: too many side-lobes could cause problems).

An isotropic radiator (O dB_igain) placed in free-space between the ionosphere and the earth's surface is transformed according to surroundings, into an antenna possessing high gain if the "reflectors", earth and ionosphere, mutually aid each other. For this reason the question of the gain of a short-wave antenna has more of an academic rather than a practical value. The determined values become sterile numbers which can only be regarded with a great deal of scepticism, especially when the person undertaking the measurements does not possess a full understanding of antenna physics.

Until now, no perfectly exact calculations, let alone perfectly exact measurements of gain of practical antennas, have been carried out. Such a project would represent a very large outlay in terms of measurement and mathematical capabilities. For this reason, one must rely on approximations, which of course, cannot be regarded as being exact. If methods of calculation leading to uncertainties of several tenths or hundredths of a decibel, how can exact measurements turn out so correct?

The employment of exact mathematical calculating techniques would certainly ensure more precise results than would be obtained by practical measurement. On the other hand, the realisation of a mathematical antenna model is not possible owing to the many unknown factors such as earth inductivity and dielectric constant together with the local topography. It remains in the realm of measurements to obtain a picture of the actual conditions but these would not be carried out with accuracies of a few tenths of a decibel but more like accuracies of $\pm$ 2 to $\pm$ 5 dB.

The following CCIR-measurement uncertainties are permitted: –

10 kHz ..... 300 MHz: $\pm$ 2 dB
300 MHz ..... 3 GHz: $\pm$ 3 dB
3 GHz ..... 30 GHz: $\pm$ 5 dB

These recommendations of the international radio advisory committee speak for themselves. They were aware of the difficulties which the higher demands upon accuracy would have brought with them.

If after an approximation, the antenna gain from the main lobe of the radiation characteristic (half-power points of the E and H planes) should be determined, one conciously took inaccuracies into account; it would be totally out of place, if the results were expressed as accurate to two decimal places. In principle, there is a relationship between the antenna gain and its beamwidth, which is exclusively limited to antennas having a rotationsymmetrical main lobe or antennas where the deviation from the rotationsymmetry is in accordance with theoretical principles. Even then, it is risky to determine the gain solely from the main lobe characteristic. It is particularly delicate, when one maintains, that the gain of short-wave antennas can only be determined from the horizontal beamwidth. This is especially true in some cases where an unsymmetrical horizontal characteristic and differences in the vertical directional diagram are apparent.

It is a particularly bad mistake to ignore the vertical directional characteristic, since it is well known, that this is of quite special importance in the short-wave region in connection with the ionosphere and its reciprocal action with the earth's surface. All gain measurements which do not take the **total** radiation characteristic into account are therefore anything but precise. On this basis of a single field strength measurement, it is impossible to reach a conclusion about the gain of an antenna. To determine the exact gain the **complete space** diagram of an antenna must be taken into account.

This means: field strength measurements must be taken in all space orientations about the antenna in order to arrive at an exact and reliable result. It is possible to understand these basic points easily if one imagines that the light-intensity outside the beam of a spot-lamp falls very sharply and a few degrees further from the maximum it falls to zero. Naturally, the main beam of a radio wave is not visible and can easily be missed

in a field intensity measurement of the HF antenna, thus giving a result, which in a true sense of the word, is beside the point. An amateur wishing to make accurate field measurements must be prepared to spend at least DM 20.000,– –. The accuracy of such measurements will be in the region of ± 0,6 dB.

The following considerations, limited to gain estimates, show that the deviation of the gain from the antenna main lobe even looking at both planes of radiation, cannot be much more than a rule of thumb.

Under the condition that the definition of antenna gain is borne in mind, the notion of directivity will be used for a rough estimate of antenna gain from now on.

The directivity is defined as the relationship between the maximum radiation intensity to that of the median intensity. For an antenna with an efficiency of 100 % and no copper-, dielectric- or matching losses, the directivity and gain are equal. The equation for the estimation of the directivity is: –

(1) $$D \approx 41253 / (a\beta)$$

where the number 41253 represents the surface of a unity sphere in square units. a and β are defined angles of the plane perpendicular to the vertical radiation plane.

This formula represents a very simple approximation indeed for the calculation of the directivity of a single lobe polar plot. This formula was developed – and this is reiterated – for the rough estimation of the directivity from a knowledge of the half-power points of the radiation lobes of two 90° planes in quadrature. The half-power points are in accordance with the horizontal and vertical beamwidths and describe the widths of the radiation lobes, at which the field strength right and left from the maximum fall by 3 dB.

The constant 41253 is the subject of much misunderstanding in amateur literature and it should be made clear that this calculation method is only an approximation and it seems to be urgently necessary to explain in detail the derivation of the directivity formula.

The directivity D is defined as: the relationship of the field strength $Ø_{max}$ of the main lobe direction of the antenna at the distant point, to its median field strength $Ø_O$ which would be produced if the total radiated power P_S was not directed, but uniformaly distributed at the surface of a sphere $4\pi r^2$. Since the unity sphere has a radius of r = 1 the spherical angle becomes 4π . In the first instance, the directivity amounts to

(2) $$D = Ø_{max}/Ø_O$$

The median radiation intensity $Ø_O$ is coupled with the radiation power P_S through the relationship:

(3) $$Ps = 4\pi r^2 Ø_O$$

and transposing:

(4) $$Ø_O = P_s/4\pi r^2$$

and substituting

(5) $$D = Ø_{max}\, 4\pi r^2/P_s$$

$P_s/Ø_{max}$ id defined as B. The B represents the equivalent aperture of an idealised directivity characteristic, which has in the radiation range, the constant intensity $Ø_{max}$, and in the remaining range of angles the radiation intensity of Ø = 0. From the previous formula follows:

(6) $$B = \frac{4\pi r_2 Ø_o}{Ø_{max}\,[\text{rad}^2]}$$

i. e. a result in radians squared. The radian (rad.)

is the plane angle for which the relationship of length of the arc to its radius equals one. One radian equals an angle of 57,295° as will now be described. The circumference of the unity sphere is:

$$C = \pi d = 2\pi r, \text{ since } 2\pi r = 360°,$$
$$r = 360°/2\pi = 180°/\pi = 57{,}295°.$$

So for the surface area of the sphere S_o in square units

(7)
$$S_o = 4\pi r^2 = 4\pi (57{,}295)^2 = 41253 \text{ (degrees}^2\text{)}$$

The number 41253 is nothing more than the surface area of a unity sphere expressed in degrees squared.
In square units

(8)
$$B = \frac{41253\, \Omega_o}{\Omega_{max}\ [\text{degrees}^2]}$$

and since $\Omega_{max}/\Omega_o = D$

$$B = 41253/D \text{ and } D = 41253/B$$

As B only approximates the product of angles (half power width) in the E plane (horizontal) α and the H plane (vertical) β or in the perpendicular to the vertical plane:

$$D \approx 41253/(\alpha\, \beta)$$

reference to the isotopic radiator.

To be able to give the roughly estimated power gain in dB, the following formula is employed:

(9)
$$G(dB) = 10 \log_{10} D$$

This formula gives the gain relative to an isotropic radiator. To obtain the gain in dB with reference to a half-wave dipole 2,15 dB must be subtracted.

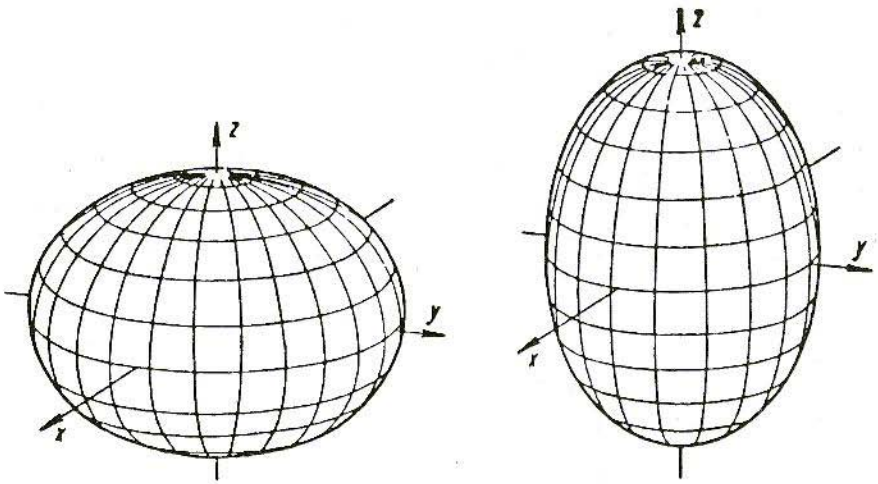

Fig. 1: 3 D radiation plot of directive antennas are similar to the form of squashed or elongated rotation ellipsoids

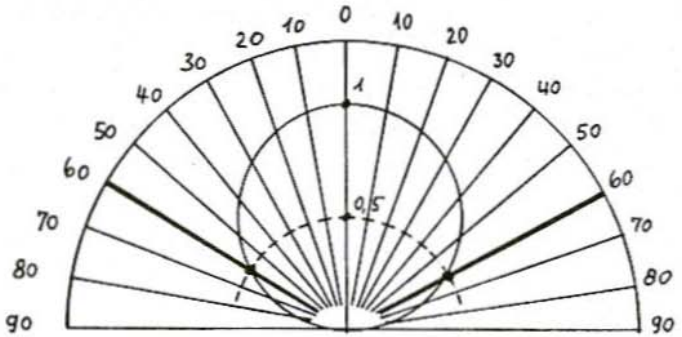

Fig. 2:
Directive antenna polar plot showing half-power points. For this semi-circular plot it amounts to 120°.

The main lobe characteristics can be calculated exactly and it is useful to compare this with the result arrived at by using the approximations formula.

The calculation of the volume of complicated bodies, such as the lobe of an antenna, is done with the aid of multiple integration. The form of a lobe is very similar to those of a squashed or elongated rotational ellipsoid. (**Fig. 1**).

In the first approximation, the antenna lobe is regarded as being rotationally symmetrical in polar co-ordinates about the pole axis rotating area of the form:

(10) $$\varnothing = \varnothing_{max} \cos^n \alpha$$

where $\varnothing$ is the radiation intensity, $\varnothing_{max}$ is the maximum radiations intensity, n is a real number and α is the radiation angle. For the main beam direction $\alpha = 0$. The aim is to calculate the volume of a radiating body possessing bent co-ordinates and is obtained by triple intregrals, whose integration area by constant co-ordinate area is separated into volume elements. The calculation of the radiation of a single beamed $\cos^n$-lobe can be reduced owing to its simplicity, to a double integral of the form:

(11) $$P_s = \iint S_r \, df$$

where P_s is the radiated power, S_r is the real part of the Poynting vector ($S_r = \frac{1}{2} \cdot EH$) of this distant field and df is a limiting value of an infinately small spherical area element.

In the following text, only side-lobe free polar-dia gram examples are considered, the calculated values being the theoretical maximum values. The antenna gain (dB) may be obtained from the directivity D by means of (9).

Using three examples, it will be proved mathematically where the blind use of the directivity formula leads.

Example 1

An antenna has an $\alpha = \beta = 120°$ i. e. 3 dB beam width in the E plane (horizontal) as well as in the H plane (vertical). The exact calculation according to **fig. 2**.

(12) $$P_s = \int_0^{2\pi} \int_0^{\pi/2} \varnothing_{max} \cos\alpha \sin\alpha \, d\alpha \, d\beta$$

(13) $$P_s = \pi \varnothing_{max}$$

If the power in **fig. 1** is considered as being radiated from an isotropic source, then both may be compared:

(14) $$\pi \varnothing_{max} = 4\pi \varnothing_o$$

and for the isotropic radiator

(15) $P_s = 4 \pi \varnothing_o$

as the radiated power for the isotropic is

$$P_s = \int_{ISO.} \varnothing_o d\Omega = \varnothing_o \int d\Omega = 4 \pi \varnothing_o$$

from which the directivity may be obtained

(16) $\varnothing_{max}/\varnothing_O = 4 \pi/\pi = 4 = D$

(17) $G = 10 \log D = 6 dB_i$

If the directivity is now calculated by use of the approximations formula.

(18) $D = 41253 \text{ grad}^2/(120° \times 120°) = 2,86$

(19) $G = 10 \log D = 4,56 dB_i$

The error is considerable.

Using the approximation method leads to an error of some 40 % low.

Example 2

An antenna has radiation angles $\alpha = \beta = 90°$ (about that of a 3 element quad).
The exact calculation is as follows: –

(20) $P_s = \varnothing_{max} \int_0^{2\pi} \int_0^{\pi/2} \cos^2\alpha \sin\alpha \, d\alpha \, d\beta$

(21) $P_s = 2 \pi \varnothing_{max}/3$

referred to an isotropic radiator

(22) $2 \pi \varnothing_{max}/3 = 4 \pi \varnothing_o$

(23) $\varnothing_{max}/\varnothing_o = 4 \pi 3/(2\pi) = 6 = D$

(24) $G = 10 \log D = 7,78 dB$

Using the approximation:

(25) $D = 41253 \text{ grad}^2/(90° \cdot 90°) = 5,09$

A result which is about 20 % lower than the correct result.

Example 3

This time $\alpha = \beta = 75°$ (approx. a 3 element yagi)

(26) $P_s = \varnothing_{max} \int_0^{2\pi} \int_0^{\pi/2} \cos^3 \alpha \sin \alpha \, d\alpha \, d\beta$

(27) $P_s = \pi \varnothing_{max}/2$

If P_s, again, is referred to an isotopic radiator:

(28) $\pi \varnothing_{max}/2 = 4 \pi \varnothing_o$

(29) $\varnothing_{max}/\varnothing_o = 4 \pi 2/\pi = 8 = D$

Using the approximations formula:

(30) $D = 41253 \text{ grad}^2/(75° \cdot 75°) = 7,33$

This time the approximations formula is about 9 % lower than the precise result.

From these examples it may be concluded that the approximations method used for the range of angles associated with simple amateur antennas, is hardly usable since it does not supply exact results. Even under the condition that the beamwidth is exactly known (which is unlikely) the directivity formula can only supply a "rule of thumb" result.

The main lobe is only one of the gain determining factors of the antenna. Another important factor is the size of the nearest side-lobe maxima, which has been more or less ignored by the approximations formula.

The relationship of side-lobe to main-lobe depends upon the form of the radiator and its method of excitation. It is a fallacy, that antennas possessing many side-lobes are mostly dependent upon the main lobe for the total directivity. It

is a fact that a parabolic antenna possessing many side-lobes may have a directivity which has been enhanced by up to 50 % by them. The consequence is, that antennas which have exactly the same beam-width in the main lobe could have very different gains. Although it is quite possible that in some cases – perfectly fortuitous – the approximations may approach the exact gain of the antenna, this cannot be physically proved.

Also in the case of short-wave antennas there is no relationship between the reduction of gain and the side-lobe attenuation which is generally accepted. This is also true of Yagi antennas, as the parameter upon which the side-lobes maxima depend, such as current distribution, phase relations ships, antenna length, spacing of elements and so on, is different for each antenna. All attempts at a graphical representation to arrive at an estimation of gain, be taking into account the side-lobes, are doomed to failure. That is why in serious puplications, no such graphical representations are to be found. For certain types of antennas this type of graph could be useful in order to control the construction of the antenna.

There still remains the possibility of determining the antenna gain by graphical integration. This has a pre-condition that the measurement techniques are up to the task of producing an accurate polar diagram.

Henry Jasik gives a formula in Antenna Engineering Handbook which will estimate an antenna gain: –

(31) $$G \approx 27000\ (\alpha\beta)$$

where α and β are the half-power angles in the E and H plane. Jasik also says: "It is sometimes of interest to determine a roughly estimates value of the gain if the only known data are the principle planes of the polar plot." About the formula itself, he says: "The gain found by this method is usually correct to within 25 %, particularly for high-gain-antennas". Jasik continues: "The gain can often be determined from the directivity by estimating the losses in the antenna system, but it is usually measured experimentally by direct comparison methods. The only additional advice, which the author can supply is, that the measurement of total gain is probably the most difficult measurement of antenna technology. It should only be undertaken with great care".

Finally, Proffessor G. Beuche DL6AB wrote in QRV 6/79 his contribution to the theme: "Origin, meaning and conditions of this relationship (note: he means the approximations formula) are unknown probably, by many authors of amateur puplications, otherwise this terrible confusion would not have arisen.

References

1 Jasik, Henry: Antenna Engineering Handbook, McGraw-Hill 1961
2 Kraus, John D.: Antennas, McGraw-Hill 1950
3 Hock, Albrecht u. a.: Hochfrequenzmesstechnik 1 und 2
Lexika-Verlag, Grafenau/Württ., sowie
expert Verlag Grafenau/Württ. 1980
4 Stirner, Edmund: Antennen, Band 1 und 2,
Dr. Alfred Huethig Verlag Heidelberg, 1980
5 Meinke, H. und Gundlach, F. W.: Taschenbuch der Hochfrequenztechnik,
Springer-Verlag Berlin/Goettingen/Heidelberg 1962
6 Stein, V. und Raab, M.: Gutachten Amateurfunkantenne Periodic 5,
Deutsche Forschungs- und Versuchsanstalt für Luft- und Raumfahrt e. V.,
Oberpfaffenhofen, August 1982 (unveröffentlicht)
7 Laport, E. A.: Radio-Antenna Engineering, McGraw-Hill, N. Y. 1952
8 Henss, P.: Strahlungsmessungen an Rundfunk- und TV-Antennen mit einem Hubschrauber,
Neues von Rohde u. Schwarz 79, Herbst 1977
9 Jäger, G.: Einfluß des Erdbodens auf Antennendiagramme,
Int. Elektronische Rundschau 1960, Heft 4
10 Schelkunoff, S. A. und Friis, H. T.: Antennas, Theory and Practice,
John Wiley, N. Y. 1952

MATERIAL PRICE LIST OF EQUIPMENT

described in edition 3/85 of VHF COMMUNICATIONS

DC9XG	**GaAs-FET Inter-Locked Dual Polarity Power Supplies for portable Use**		Art. No.	**Ed. 3/1985**
PC-board	DC9XG 001	single-sided, drilled with comp. plan	6925	DM 27.—
Components	DC9XG 001	4 ICs, 3 transistors, 7 diodes, 11 elkos, 7 foil-, 5 ceramic and 2 styro flex-caps. 3 presets, 15 resistors, tin-plate case	6926	DM 62.—
Kit	**DC9XG 001**	**complete, with above parts**	**6927**	**DM 85.—**
DB1NV	**Stable Crystal-Controlled-Source for 10,37 GHz**			**Ed. 3/1985**
PC-board	DB1NV 003	double-sided, silvered without layout plan, undrilled	6928	DM 24.—
Components	DB1NV 003	5 transistors, 2 diodes, 1 regulator 1 coil-former with core, 14 trimmers, 3 chokes, 1 m silvered 1 mm wire, 3 elkos, 2 foil- and 18 disc caps. 21 resistors, 1 preset, 1 W/G R 100, 80 mm long	6929	DM 103.—
Crystal	96,000 MHz	HC-25U or HC-43U	6224	DM 26.—
Step-recovery-diode		HP5082-0830	6930	DM 260.—
Kit	**DB1NV 003**	**complete , with above parts**	**6931**	**DM 395.—**
DB1NV	**12-V-Mobile-Switched.-Mode-Power-Supply (10 A cont., 20 A int.)**		**Art. No.**	**Ed. 2-3 / 85**
PC-board	DB1NV 002	single-sided with comp. plan, drilled	6932	DM 83.—
Components	DB1NV 002	upon request		
DTK	**FM-AM-Converter for FAX Reception**			**Ed. 3/1985**
PC-board	DTK 001	single-sided with comp. plan, drilled	6921	DM 28.—
Components	DTK 001	5 ICs, 1 transistor, 1 Z-diode 1 foil trimmer, 6 elkos, 6 foil and 16 ceramic capacitors, 3 presets (upright), 28 resistors, 5 solderpins	6922	DM 77.—
Crystal	2,4576 MHz	HC-6U	6923	DM 18.—
Kit	**DTK 001**	**complete, with above parts**	**6924**	**DM 119.—**

UKWberichte Terry D. Bittan · Jahnstr. 14 · Postfach 80 · D-8523 Baiersdorf
Tel. West Germany 9133-855. For Representatives see cover page 2

Space and Astronomical Slides

Informative and Impressive

VHF COMMUNICATIONS now offers sets of phantastic slides made during the Gemini,Apollo,Mariner, and Voyager missions, as well as slides from leading observatories. These are standard size 5 cm x 5 cm slides which are framed and annotated.

Prices plus DM 3.00 for post and packing.

Sets of 5 NASA-slides DM 8.50 per set

Set 8103	Apollo 11: Earth and Moon
Set 8104	Apollo 11: Man of the Moon
Set 8105	Apollo 9 and 10: Moon Rehearsal
Set 8106	From California to Cap Canaveral
Set 8107	Apollo 12: Moon Revisited
Set 8108	Gemini Earth Views
Set 8109	Apollo 15: Roving Hadley Rille
Set 8110	Apollo 16: Into the Highlands
Set 8111	Apollo 17: Last voyage to the moon
Set 8112	Apollo 17: Last Moon Walks
Set 8113	Mariner 10: Mercury and Venus

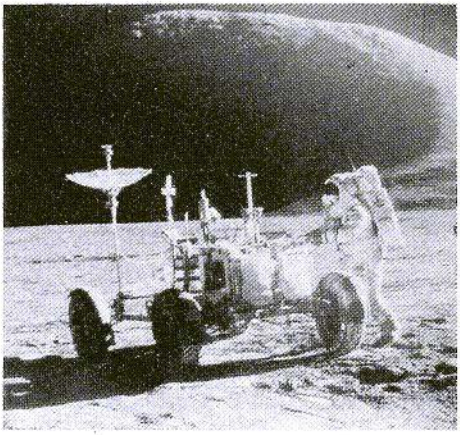

Set 8147 »Jupiter encountered« 20 slides of VOYAGER 1 & 2 DM 35.00

1. Jupiter and 3 satellites 2. The giant planet 3. Jupiter, Io and Europa 4. The Red spot 5. The Red spot in detail 6. The swirling clouds 7. Io and a white oval 8. The neighbourhood of the Red spot 9. The rings of Jupiter 10. The Gallilean satellites 11. Amalthea 12. Callisto 13. Impact feature on Callisto 14. Eruption on Io 15. Io full disc 16. Europa close-up 17. Europa distant view 18. Ganymede close-up 19. A distant Ganymede 20. The Iovian system

Set 8100 »Saturn encountered«, 20 VOYAGER-1 slides DM 35.00

1. Saturn and 6 of its moons 2. Saturn from 11 mio miles 3. Saturn from 8 mio miles 4. Saturn from 1 mio miles 5. Saturn and rings from 900.000 miles 6. Saturn's Red spot 7. Cloud belts in detail 8. Dions against Saturn 9. Dione close-up 10. Rhea 11. Craters of Rhea 12. Titan 13. Titan's polar hood 14. Huge crater on Mimas 15. Other side of Mimas 16. Approaching the rings 17. Under the rings 18. Below the rings 19. »Braided« F ring 20. Iapetus

Set 8148 »VOYAGER 2 at Saturn«, 20 VOYAGER-2 slides DM 35.00

1. VOYAGER 2 approaches 2. Clouds & rings 3. Storms & satellites 4. Cyclones, spots & jet streams 5. Convective regions 6. Atmospheric disturbance 7. Rings & shadows 8. The »C« ring 9. Ring details 10. The »A« ring 11. Looking back on Saturn 12. Titan – night side 13. Titan – atmospheric bands 14. The »F« ring 15. Hyperion close-up 16. Iapetus revealed 17. Enceladus explored 18. The Tethys canyon 19. The »F« ring structure 20. Within the Enke division

Set 8102 »The Solar System«, 20 NASA/JPL slides DM 35.00

1. Solar System 2. Formation of the Planets 3. The Sun 4. Mercury 5. Crescent Venus 6. Clouds of Venus 7. Earth 8.Full Moon 9. Mars 10. Mars: Olympus Mons 11. Mars: Grand Canyon 12. Mars: Sinuous Channel 13. Phobos 14. Jupiter with Moons 15. Jupiter Red Spot 16. Saturn 17. Saturn Rings 18. Uranus and Neptune 19. Pluto 20. Comet Ikeya-Seki.

Set 8149 »The Sun in action«, 20 NASA/JPL slides DM 35.00

1. Sun in H-α light 2. Total Solar eclipse 3. Outer corona 4. Corona from SMM satellite 5. Corona close-up 6. Solar magnetogram 7. Active regions in X-radiation 8. X-ray corona 9. A coronal hole 10. Solar flare 11. Active Sun 12. Eruptive prominence 13. Gargantuan prominence 14. Eruptive prominence 15. Huge Solar explosion 16. Prominence in action 17. Sun in action 18. Magnetic field loops 19. Prominence close-up 20. Chromospheric spray

Set 8144 »Space shuttle«, 12 first-flight slides DM 24.00

1. STS1 heads aloft 2. View from the tower 3. Tower clear 4. Launch profile 5. Payload bay open 6. STS control Houston 7. In orbit, earth seen through the windows 8. Bob Crippen in mid-deck 9. John Young 10. Approaching touchdown 11. After 54.5 hours in space Columbia returns to Earth. 12. Astronauts Crippen and Young emerge after the successful mission

Set 8150 »Stars and Galaxies«, 30 astro color slides, AAT 1977 – 1982, DM 46.00

1.The Anglo-Australian 3.9 m Telescope (AAT) 2.AAT Dome 3.Telescope Control Console 4.An Observer at the Prime Focus 5.Star Trails in the SW 6. Circumpolar Star Trails 7.Centaurus A.NGC5128 8.The Spiral Galaxy M83 (NGC5236) 9.The Eta Carinae Nebula 10.An open Cluster of Stars NGC3293 11.A Planetary Nebula, NGC6302 12.The Trifid Nebula M20 (NGC6514) 13.The Cone Nebula 14.S Monocerotis and NGC2264 15.The Helix Nebula.NGC7293 16.A Wolf-Rayet Star in NGC2359 17.A Spiral Galaxy,NGC2997 18.Messier 16 (NGC6611) 19.The Orion Nebula 20.Dust and Gas in Sagittarius,NGC6589-90 21.NGC6164/5, The Nebulosity Around HD148937 22.Dust Cloud and Open Cluster NGC6520 23.The Spiral Galaxy NGC253 24.A Mass-Loss Star, IC2220 25.The Jewel Box NGC4755 26.Local Group Galaxy NGC6822 27.Central Regions of NGC5128 28.Towards the Galactic Centre 29.The Trapezium 30.The Trifid Stars

UKW*berichte* Terry D. Bittan · Jahnstr. 14 · Postfach 80 · D-8523 Baiersdorf
Tel. West Germany 9133-855. For Representatives see cover page 2

You should know what's behind our sign

We are the only European manufacturers of these

Miniature TCXO's

CCO 102, CCO 103, CCO 104, CCO 152 modulable table

- higher stability than a quartz crystal: less than ± 3 ppm over the temperature range –30 to +60°C. (types B)
- low ageing rate: less than 1 ppm per year.
- wide frequency range: 10 MHz to 80 MHz
- low supply voltage: +5 V
- low current consumption: 3 mA max. (series CCO 102)
- small outlines: CCO 104 = 2,6 cm³, CCO 102/152 = 3,3 cm³, CCO 103 = 4,0 cm³
- widespread applications e.g. as channel elements or reference oscillators in UHF radios (450 and 900 MHz range)

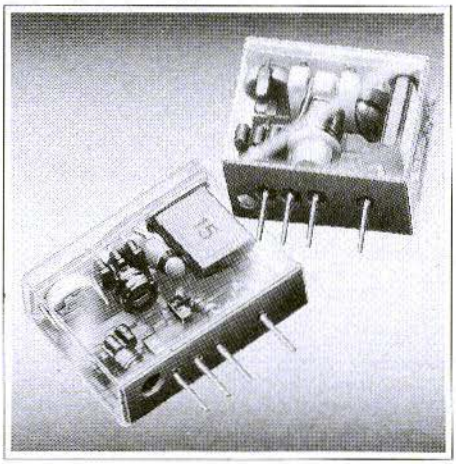

Our R + D engineers are constantly working with new technology to develop new products. We can offer technical advice for your new projects or manufacture against your specification.

Quartz crystal units in the frequency range from 800 kHz to 360 MHz Microprocessor oscillators (TCXO's, VCXO's, OCXO's) crystal components according to customer's specifications

Types	CCO 102			CCO 103			CCO 104		
	A	B	F	A	B	F	A	B	F
Freq. range	10 – 80 MHz			6.4 – 25 MHz			10 – 90 MHz		
stability vs temp. range	–30 to +60°C			–30 to +60°C			–30 to +60°C		
Current consumption	max. 3 mA at UB = +5 V			max. 10 mA at UB = +5 V			max. 10 mA at UB = +5 V		
input signal	–10 dB/50 Ohm			TTL-compatible (Fan-out 2)			0dB/50 Ohm		

CCO 152 A + B

same size as CCO 102 A + B

modulation input:	
deviation:	typ. 1 kHz/V
mod. frequency:	DC to 10 kHz
impedance:	20 k Ohm

TELE QUARZ

... Your precise and reliable source

TELE-QUARZ GMBH · D-6924 Neckarbischofsheim 2
Telefon 0 72 68/10 03 · Telex 782359 tq a · Telefax 07268/1435